

1-15-2014 12:00 AM

# miRNA Regulation of Programmed Cell Death-1 in T Cells: Potential Prognostic and Therapeutic Markers in Melanoma

Nathan J. Johnston, *The University of Western Ontario*

Supervisor: Dr. Weiping Min, *The University of Western Ontario*

A thesis submitted in partial fulfillment of the requirements for the Master of Science degree in  
Pathology

© Nathan J. Johnston 2014

Follow this and additional works at: <https://ir.lib.uwo.ca/etd>



Part of the [Biological Phenomena, Cell Phenomena, and Immunity Commons](#)

---

## Recommended Citation

Johnston, Nathan J., "miRNA Regulation of Programmed Cell Death-1 in T Cells: Potential Prognostic and Therapeutic Markers in Melanoma" (2014). *Electronic Thesis and Dissertation Repository*. 2674.  
<https://ir.lib.uwo.ca/etd/2674>

This Dissertation/Thesis is brought to you for free and open access by Scholarship@Western. It has been accepted for inclusion in Electronic Thesis and Dissertation Repository by an authorized administrator of Scholarship@Western. For more information, please contact [wlsadmin@uwo.ca](mailto:wlsadmin@uwo.ca).

**miRNA REGULATION OF PROGRAMMED CELL DEATH-1 IN T CELLS:  
POTENTIAL PROGNOSTIC AND THERAPEUTIC MARKERS IN MELANOMA**

Thesis format: Monograph

by

Nathan Joseph Johnston

Graduate Program in Pathology

A thesis submitted in partial fulfillment  
of the requirements for the degree of  
Master of Science

The School of Graduate and Postdoctoral Studies  
The University of Western Ontario  
London, Ontario, Canada

© Nathan Joseph Johnston 2015

## Abstract

Immunoinhibitory cell receptors that can induce a state of T cell exhaustion upon exposure to tumor antigen include Programmed Cell Death-1 (PD1). Although much research has been conducted on PD1, global miRNA regulation of PD1 in a cancer model has not been investigated. We hypothesized that miRNAs exist that can silence PD1 *in vitro* and revert symptoms of T cell exhaustion. Eleven miRNAs were discovered with altered expression between PD1<sup>+</sup> and PD1<sup>-</sup> CD4<sup>+</sup> T cells from melanoma-bearing mice. miR-28 and miR-107 mimics were shown to bind to and silence the 3'UTR of PD1, and miR-28, miR-150 and miR-107 inhibitors increased PD1 expression. Furthermore, no changes were observed in anti-CD3e induced proliferation, while miR-28 and miR-107 mimic transfection significantly reduced activation-induced apoptosis. This study is the first of its kind to discover global miRNA profiles in PD1<sup>+</sup> T cells, providing novel targets for potential use as prognostic and therapeutic markers in melanoma.

## Keywords

Programmed Cell Death-1, T cell exhaustion, melanoma, RNA interference, T cells, microRNA-28, microRNA-150, microRNA-103, microRNA-107

# Acknowledgments

With 2 years of my life devoted to my MSc I have received a lot of support for which I am thankful for. I would like to dedicate this thesis to my supervisors, technician, committee advisors, co-researchers, and Department of Pathology professors and administrative staff.

My supervisors were a blessing and provided me with a nurturing environment to pursue my research interests. Drs. Weiping Min and Xiufen Zheng respected me as a researcher and granted me independence in my research goals. Their support was extremely appreciated and made me tremendously happy that I chose to pursue my MSc in their lab.

Next, I would like to acknowledge Xusheng Zhang, our lab technician that has provided most of my knowledge in laboratory techniques and has gone above and beyond to ensure success in my project. I'm quite positive that without his presence I would not have grown to be the researcher I am today.

Two others that deserve acknowledgement are the members of my advisory committee, Drs. Jim Koropatnick and Subrata Chakrabarti. Even though the meetings were far and few between, each word they uttered unequivocally helped shape the research questions I needed to ask to create a novel project. Their advice also extended towards my future goals and provided me with an insight into research that aided in my decision to pursue a PhD degree.

As well, throughout my two years in the Min laboratory I have been lucky enough to meet a multitude of graduate and undergraduate students, postdocs and medical students and residents that have participated in the adventures of graduate research. This group of individuals has each had their part in making my graduate journey exciting.

I would also like to acknowledge Drs. Zia Khan and Chandan Chakraborty. Participating in their journal club and grant writing classes taught me extensive analytical and critical thinking skills necessary to become an above-and-beyond researcher. Their teachings granted me a proper transition into the graduate student mindset and helped shape my thesis in a meaningful way.

Lastly, my acknowledgements would not be complete without mentioning the wonderful Department of Pathology administrative staff: Tracey, Susan, Kathilyn, Cecille and Mair. One in particular, Tracey Koning, went above and beyond to answer all the questions I had about various administrative issues.

I will forever have great memories of all your support and guidance. Having spent 6 years learning at Western University, this group of people has solidified my belief that the Department of Pathology is the best department at Western.

# Table of Contents

Title .....	i
Abstract .....	ii
Acknowledgments.....	iii
Table of Contents .....	iv
List of Tables .....	vii
List of Figures .....	viii
List of Abbreviations .....	x
<b>Chapter 1</b> .....	<b>1</b>
1 Introduction .....	1
1.1 Melanoma and epidemiology .....	1
1.1.1 Current treatment strategies .....	2
1.2 T cell exhaustion .....	3
1.2.1 Inhibitory cell receptors linked to T cell exhaustion .....	5
1.2.2 Clinical immunotherapies .....	7
1.3 Epigenetics .....	7
1.4 RNA interference and microRNAs .....	8
1.5 miRNAs reported in melanoma.....	9
1.5.1 Prognostic potential .....	9
1.5.2 Therapeutic potential .....	10
1.6 microRNAs in T cell exhaustion .....	11
1.7 Rationale.....	11
1.8 Hypothesis .....	11

1.9	Specific aims .....	12
<b>Chapter 2</b>	.....	13
2	Materials and methods .....	13
2.1	B16F10 cell culture .....	13
2.2	Melanoma mouse model .....	13
2.3	Lymphocyte isolation .....	14
2.3.1	Lymphocyte isolation from lymph nodes .....	14
2.3.2	Lymphocyte isolation from spleen.....	14
2.3.3	Lymphocyte isolation from tumor tissue .....	14
2.4	Flow cytometry and cell sorting.....	15
2.5	miRNA extraction and cDNA synthesis .....	15
2.6	mRNA extraction and cDNA synthesis.....	16
2.7	miRNA array analysis .....	17
2.8	Real-time quantitative PCR.....	19
2.9	<i>In silico</i> analysis .....	22
2.10	pmirGLO dual luciferase plasmid .....	22
2.10.1	PD1 3' UTR amplification.....	22
2.10.2	Restriction enzyme digestion and ligation.....	24
2.10.3	Amplification and sequencing .....	24
2.10.4	Plasmid and miRNA mimic transfection .....	25
2.10.5	Dual Luciferase Assay .....	27
2.11	Lymphocyte treatment with anti-CD3e and IFN $\gamma$ .....	28
2.12	T cell transfection with siRNA, miRNA mimics and inhibitors .....	28
2.13	Analysis of proliferation and apoptosis using flow cytometry.....	30
2.14	Statistical analysis .....	31

<b>Chapter 3</b> .....	32
3 Results .....	32
3.1 PD1 displays increased expression in T cells isolated from lymphoid and tumor tissue in a B16F10 mouse melanoma model .....	32
3.2 11 miRNAs have altered expression in PD1 <sup>+</sup> CD4 <sup>+</sup> T cells.....	32
3.3 <i>In silico</i> analysis of miRNAs that may bind to the 3' UTR of PD1, TIM3 and BTLA.....	35
3.4 miR-28 and miR-107 silence PD1 through its 3' UTR.....	35
3.5 Anti-CD3e, but not IFN $\gamma$ , upregulates PD1 and BTLA expression <i>in vitro</i> .....	46
3.6 miR-28, miR-150, miR-103 and miR-107 show decreased expression after anti-CD3e treatment .....	53
3.7 miR-28 and miR-107 inhibitors increase PD1 expression in CD4 <sup>+</sup> T cells <i>in vitro</i> .....	53
3.8 miR-28 and miR-107 mimic transfection has no effect on proliferation in CD4 <sup>+</sup> T cells. ....	60
3.9 miR-28 mimic transfection reduces anti-CD3e induced early and late apoptosis in CD4 <sup>+</sup> T cells.....	69
<b>Chapter 4</b> .....	72
4 Discussion .....	72
4.1 Discussion .....	72
4.2 Future Directions.....	78
<b>Chapter 5</b> .....	80
5 References .....	80
<b>Curriculum Vitae</b> .....	92

## List of Tables

Table 2.1 Affymetrix GeneChip 3.0 miRNA Array miRNA probe sequences .....	18
Table 2.2 Target sequences of miRNA primers for real time qPCR analysis .....	20
Table 2.3 Primers used in RT-qPCR detection of mRNA levels.....	21
Table 2.4 PD1 3' UTR primer sequences .....	23
Table 2.5 miRNA mimic sequences / miRNA inhibitor targets .....	26
Table 2.6 Small interfering RNA sequences.....	29
Table 3.1 miRNA candidates that may silence PD1, TIM3 and BTLA in various combinations .....	42



## List of Figures

Figure 3.1 CD4 <sup>+</sup> and CD8 <sup>+</sup> T cells from lymph nodes, spleens and tumors of B16F10 tumor-bearing mice express significantly more PD1 than T cells from WT mice .....	33
Figure 3.2 19 miRNAs have significantly altered expression between CD4 <sup>+</sup> PD1 <sup>-</sup> and CD4 <sup>+</sup> PD1 <sup>+</sup> T cells isolated from tumor-bearing mice .....	36
Figure 3.3 Fold changes in miRNA expression between PD1 <sup>+</sup> CD4 <sup>+</sup> and PD1 <sup>-</sup> CD4 <sup>+</sup> T cells determined by the miRNA array and qPCR data .....	38
Figure 3.4 RT-qPCR confirms 11 significantly up- and downregulated miRNAs discovered in the microRNA array .....	40
Figure 3.5 Candidate miRNA alignment on the 3' UTRs of PD1, BTLA and TIM3 mRNA. ....	44
Figure 3.6 miR-28 and miR-107 bind to and silence the PD1 3' UTR .....	47
Figure 3.7 Anti-CD3e treatment increases PD1 and BTLA expression in a dose-dependent manner .....	49
Figure 3.8 IFN $\gamma$ treatment has no effect on PD1, TIM3 or BTLA expression .....	51
Figure 3.9 miR-28, miR-150, miR-103 and miR-107 decrease expression after PD1 upregulation mediated by anti-CD3e binding .....	54
Figure 3.10 Lipofectamine 2000 demonstrates greater transfection efficiency in T cells compared to Lipofectamine .....	56
Figure 3.11 A 2:1 ratio of siRNA ( $\mu$ g):Lipofectamine 2000 ( $\mu$ L) provides the optimal T cell transfection efficiency and total viability.....	58
Figure 3.12 A 2:1 ratio of GAPDH siRNA ( $\mu$ g):Lipofectamine 2000 ( $\mu$ L) results in a 75% knockdown in GAPDH expression 48 hours after transfection .....	61

Figure 3.13 miR-28, miR-150 and miR-107 inhibitors increase PD1 expression after T cell transfection and incubation on anti-CD3e coated plates.....	63
Figure 3.14 miR-28 significantly silences PD1 expression in CD4 <sup>+</sup> T cells after transfection and incubation on anti-CD3e coated plates.....	65
Figure 3.15 miR-28 and miR-107 have no effect on cell proliferation induced by anti-CD3e stimulation .....	67
Figure 3.16 miR-28 mimic transfection significantly reduces the percentage of cells in early and late apoptosis caused by prolonged anti-CD3e activation .....	70

## List of Abbreviations

2-ME	2-mercaptoethanol
APC	Allophycocyanin
B16F10	Mouse melanoma cell line
$\beta$ -Actin	Beta-actin
Bcl-2	B-cell lymphoma 2
BLIMP-1	PR domain zinc finger protein 1
BRAF	V-RAF murine sarcoma viral oncogene homolog B
BTLA	B and T lymphocyte attenuator
C57BL/6	Mouse strain C57 Black 6
CCND1	G1/S-specific cyclin-D1
CCR7	C-C chemokine receptor 7
CD	Cluster of differentiation
CDK8	Cyclin-dependent kinase 8
cDNA	Complementary DNA
CTLA4	Cytotoxic T-lymphocyte-associated protein 4
c-Myb	Myb proto-oncogene protein
DC	Dendritic cell
DICER	Endoribonuclease dicer
DMEM	Dulbecco's modified eagle medium
DMSO	Dimethyl sulfoxide
DNMT	DNA methyltransferase
dNTP	Deoxyribonucleotide triphosphate
ERK	Extracellular signal-regulated kinases
FADD	Fas-associated death domain

FBS	Fetal bovine serum
FITC	Fluorescein isothiocyanate
GAPDH	Glyceraldehyde 3-phosphate dehydrogenase
GM-CSF	granulocyte macrophage colony stimulating factor
HDAC	Histone deacetylase
HIV	Human immunodeficiency virus
HMGB1	High-mobility group protein B1
IFN $\gamma$	Interferon gamma
Ig	Immunoglobulin
IHC	Immunohistochemistry
IL	Interleukin
IRAK1	Interleukin-1 receptor-associated kinase 1
LAMP1	Lysosomal-associated membrane protein 1
LB	Lysogeny broth
LCMV	Lymphocytic choriomeningitis virus
LPS	Lipopolysaccharide
MAD2L1	MAD2 mitotic arrest deficient-like 1
MAPK	Mitogen-activated protein kinase
MCL1	Induced myeloid leukemia cell differentiation protein Mcl-1
MEK	Mitogen-activated protein kinase kinase
miRNA	MicroRNA
mRNA	Messenger RNA
NF- $\kappa$ B	nuclear factor kappa-light-chain-enhancer of activated B cells
NK	Natural killer
NKTL	Natural killer/T-cell lymphoma

NY-ESO-1	Cancer-testis antigen
OPTI-MEM	Reduced serum cell culture medium
PBS	Phosphate buffered saline
PD1 / PDCD1	Programmed cell death-1
PDCD4	Programmed cell death protein 4
PD-L1/2	Programmed death-ligand 1/2
PE	Phycoerythrin
PTEN	Phosphatase and tensin homolog
RISC	RNA-induced silencing complex
RNAi	RNA interference
RT-qPCR	Reverse transcription quantitative polymerase chain reaction
SHIP	SH2-containing Inositol 5'-Phosphatase
SHP-1/2	Src homology region 2 domain-containing phosphatase-1/2
siRNA	Small interfering RNA
SNORD61	Homo sapiens small nucleolar RNA, C/D box 61
SOCS1	Suppressor of cytokine signaling 1
TAA	Tumor-associated antigen
TGF- $\beta$	transforming growth factor beta
TIL	Tumor infiltrating lymphocyte
TIM3	T cell immunoglobulin domain and mucin domain 3
TNF $\alpha$	Tumor necrosis factor alpha
TRAF6	TNF receptor-associated factor 6
UTR	Untranslated Region
V600E/K	Valine (V) to glutamic acid (E) or lysine (K) at position 600
VEGF	Vascular endothelial growth factor

## Chapter 1

### 1 Introduction

#### 1.1 Melanoma and epidemiology

There are three types of skin cancer, which are named from the cells they emerge from: non-melanoma skin cancers such as squamous cell carcinoma and basal cell carcinoma, and the deadliest kind known as melanoma [1]. Melanoma begins in melanocytes, the pigment producing cells in the skin, and is primarily caused through unrepaired DNA damage from ultraviolet radiation [1]. Melanocytes make up about 5-10% of all skin cells and, in humans, are distributed as single cells within the basal layer of the epidermis, while mouse melanocytes are found in the dermis in hair follicles [2]. Each melanocyte is surrounded by approximately 5 keratinocytes, but maintain contact with up to 40 surrounding keratinocytes through dendritic extensions, thus forming an epidermal melanin unit [3]. Upon exposure to sunlight, a keratinocyte signals to its connecting melanocyte to synthesize melanin in vesicles known as melanosomes. These melanosomes are transported through the dendritic connections to deposit melanin in the keratinocytes, which protects by cells from UV radiation by absorbing UV photons and removing highly reactive oxygen radicals [4]. With enough UV radiation, mutations can occur that cause melanocytes to grow out of control into a tumor. However, since melanoma can occur in areas of that body that receive little to no sunlight, it is believed that a combination of environmental and genetic factors lead to the development of melanoma.

In 2014, it is estimated that there was approximately 6,500 new melanoma cases and 1,050 melanoma-related deaths in Canada, representing 3% of new cancer cases and 1.4% of cancer deaths [1]. Over the 5 year span from 2006-2010, approximately 8% of new cancer cases affected 15-29 year old and 6% of new cases in 30-49 year olds were melanoma diagnoses [1]. Luckily, the five-year relative survival rate for melanoma is 85% and 92% in men and women, respectively [1]. However, melanoma and non-melanoma skin cancer is the most common cancer in Canada, which accounts for nearly

the same number of new cases as lung, breast, colorectal and prostate cancer combined, thus demonstrating a need to conduct further research on all aspects of melanoma treatment, diagnoses and prevention [1].

The model used in this study was a murine model of metastatic melanoma developed by subcutaneous injection of B16F10 cells. This cell line was generated in 1975 by intravenously injecting C57BL/6 mice with B16 cells, isolating pulmonary melanoma nodules and culturing the cells before injection into a new C57BL/6 mice [5]. This process was repeated 10 times to generate the metastatic B16F10 cell line that has been shown to have increased metastatic ability over parent B16F1 cells [6].

### 1.1.1 Current treatment strategies

Treatment for melanoma is quite difficult and its history demonstrates a lack of advances until the past few years. Although early-stage melanoma is easily cured, more advanced stages are quite refractory to treatment. Before the approval of Ipilimumab in 2011, no single drug or synergistic treatment demonstrated a significant increase in the overall survival rate of metastatic melanoma [7]. The first drug approved by the Food and Drug Administration (FDA) in 1975 for treatment of advanced melanoma was Dacarbazine, however the overall survival compared to placebo treatment was not significantly improved [8]. In 1995 interferon- $\alpha$ 2b became the first FDA approved immunotherapeutic agent against stage IIB/III melanoma [9] and in 1998, interleukin-2 (IL-2) became a second exogenous cytokine treatment for antitumor activity in metastatic melanoma [10]. However, use of these agents resulted in no significant increase in overall survival even though higher response rates were observed [11]. Over time it was discovered that mutations in the V-RAF murine sarcoma viral oncogene homolog B (BRAF) acted as a proto-oncogene in almost 50% of cutaneous melanomas, with the majority, almost 90%, occurring at codon 600 [12]. In 2011 and 2013, the FDA approved Vemurafenib and Dabrafenib, respectively, small-molecule inhibitors of V600E and V600K mutations for treatment of V600-mutated melanoma [13]. Unfortunately resistance develops in many patients after 6 months, demonstrating the need for newer therapies [14]. Since BRAF

works by phosphorylating MEK1 and MEK2 in the MAPK/ERK pathway [15], a small-molecule inhibitor of MEK1 and MEK2, Trametinib, was tested and approved by the FDA in May 2013 for the treatment of BRAF V600E and V600K [16]. Since January 2014, the FDA has granted accelerated approval of a combination regime of Dabrafenib and Trametinib, which has published immature data that suggests that the resistance achieved through BRAF inhibition monotherapy may be curbed with the addition of a MEK inhibitor [17]. Other targeted therapies that have been approved by the FDA for other cancers and have recently been studied in melanoma involve tyrosine kinase (c-kit and bcr-abl) and angiogenesis (VEGF) inhibitors, however the results are not as promising as BRAF/MEK inhibitors or upcoming immunotherapies [18, 19].

Currently, although localized melanoma and regional lymph node resection is the standard of care, targeting the immune system provides an indirect method to control cancer cell growth by potentiating ongoing and inefficient antitumor immune responses to break tolerance [20]. Since the approval of an anti-CTLA4 antibody in 2011 there has been a surge of interest in moving the focus of cancer research toward removing intratumoral immune suppression [20, 21]. This suppression includes the activation of inhibitory receptors such as CTLA4, PD1, TIM3 and BTLA on T cells that triggers an immune checkpoint resulting in inhibition of T cells directed against cancer antigens, thus preventing the immune system from combating the cancer [22]. This phenomenon has loosely been termed, T cell exhaustion, since these inhibitory receptors bind B7 molecules on antigen presenting cells preventing the activation of the CD28 co-stimulatory signal or they may bind various ligands on tumor cells creating a state of T cell anergy.

## 1.2 T cell exhaustion

T cell exhaustion is when T cells, in response to antigen stimulation, fail to proliferate and exert effector functions such as cytotoxicity and cytokine secretion. Exhausted T cells were initially observed in chronic lymphocytic choriomeningitis virus (LCMV) infection in mice and characterized by sustained expression of programmed cell death-1



(PD1) [23, 24]. Blockade of the PD1/PD-L1 interaction resulted in reduced spontaneous apoptosis, enhanced expansion and improved cytokine secretion of the exhausted T cells [23, 24]. T cell exhaustion also occurs in cancer; PD1 expression is associated with CD8<sup>+</sup> T cells in solid tumors and on antigen specific tumor-infiltrating CD8<sup>+</sup> T cells [25-27]. Similar to the LCMV model, blockade of PD1/PD-L1 interaction in both humans and mice resulted in enhanced cytolytic activity of tumor-associated antigen (TAA)-specific CD8<sup>+</sup> T cells and cytokine production of TAA-specific T helper cells when interacting directly with the tumor [26]. However, it is important to note that reversal of exhausted T cells does not always result from blockade of the PD1/PD-L1 interaction [27, 28]. Small interfering RNA (siRNA)-mediated knockdown of PD1 in T cells has shown to enhance their functions [29, 30], while in other cases siRNA-mediated PD1 knockdown of T cells did not affect their functions [28]. This indicates that other mechanisms and pathways are likely involved in T cell exhaustion.

One pathway that may also be involved in T cell exhaustion is the T-cell immunoglobulin and mucin-domain-containing molecule 3 (TIM3) negative regulatory pathway. CD4<sup>+</sup> and CD8<sup>+</sup> tumor infiltrating lymphocytes (TILs) in mice bearing the solid tumors for colon adenocarcinoma (CT-26), melanoma (B16) and breast cancer (4T1) coexpress TIM3 and PD1 [31]. More importantly, all TIM3<sup>+</sup> TILs co-express PD1 in these 3 cancer models [31] and TIM3<sup>+</sup>/PD1<sup>+</sup> CD8<sup>+</sup> T-cells are more dysfunctional than TIM3<sup>-</sup>/PD1<sup>+</sup> and TIM3<sup>-</sup>/PD1<sup>-</sup> CD8<sup>+</sup> T cells as can be seen by a failure to proliferate and produce IL-2, TNF $\alpha$ , and IFN $\gamma$  [31-33]. Targeting both pathways with anti-TIM3 [31, 32]/TIM3 fusion protein [33] and anti-PD-L1 antibodies resulted in reversed tumor-induced T cell exhaustion *in vitro* [32], reduced tumor growth *in vivo* [31] and reduced tumor burden and superior survival advantage *in vivo* [33] in both solid and non-solid cancers; colon adenocarcinoma [31], melanoma<sup>[32]</sup> and acute myeloid leukemia [33]. As well, the reduction of TIM3<sup>+</sup>PD1<sup>-</sup> cells was associated with an increased frequency of TIM3<sup>-</sup>PD1<sup>+</sup> cells, thus, the combinational effect of anti-TIM3 and anti-PD1 in suppressing melanoma and colon adenocarcinoma growth may lead to the maintenance of TIM3<sup>-</sup>/PD1<sup>-</sup> T cells [34]. Therefore, combined antibody blockade of the PD1/PD-L1 and TIM3 in cancer has proven to be beneficial in reducing tumor growth and T cell exhaustion.

A third pathway that may be involved in T cell exhaustion is the B and T lymphocyte attenuator (BTLA) negative regulatory pathway. BTLA<sup>+</sup>/PD1<sup>+</sup>/TIM3<sup>-</sup> and BTLA<sup>+</sup>PD1<sup>+</sup>TIM3<sup>+</sup> NY-ESO-1-specific CD8<sup>+</sup> T cells represent two dysfunctional T-cell populations, determined by decreased IL-2, TNF, and IFN $\gamma$  cytokine production over BTLA<sup>-</sup>/PD1<sup>-</sup>/TIM3<sup>-</sup> and BTLA<sup>-</sup>/PD1<sup>+</sup>/TIM3<sup>-</sup> NY-ESO-1-specific CD8<sup>+</sup> T cells [35]. Thus, BTLA<sup>+</sup>/PD1<sup>+</sup>/TIM3<sup>+</sup> TILs represent the most exhausted TILs in advanced melanoma. The triple antibody blockade of BTLA, PD1 and TIM3 increased the proliferative capacity and the frequency of cytokine producing NY-ESO-1-specific CD8<sup>+</sup> T cells compared to single and double blockades [35]. Taken together with the fact that naïve T-cells are single or double positive for BTLA and TIM3, and NY-ESO-1<sup>+</sup>, Melan-A<sup>+</sup> and Mage-A10<sup>+</sup> effector cells interact via larger numbers of inhibitory receptors [22], combinational blockade of these multiple inhibitory receptors seems to be the most efficient method to revert T cell exhaustion, stimulate naïve T cell maturity and promote anti-cancer immunity. So far, Fourcade *J et al* [32, 35] have found success with their studies on this combinational blockade in advanced melanoma *in vitro*; however, no one has attempted to observe the effects of RNA interference in a synergistic therapy against the PD1, TIM3 and BTLA pathways.

### 1.2.1 Inhibitory cell receptors linked to T cell exhaustion

PD1 is a type I transmembrane receptor and a member of the immunoglobulin superfamily [36]. As well, PD1 is a member of the CD28 family of T-cell regulators and is expressed on the surface of T-cells, B-cells, macrophages and dendritic cells (DCs) [37-40]. PD1 expression is induced upon T cell activation and upon PD-L1 and PD-L2 binding [41]. Receptors such as PD1 function by recruiting tyrosine phosphatases, including SHP-1, SHP-2 and SHIP, which are responsible for altering various B and T cell responses [38-40]. Interaction between PD1 and its ligands PD-L1/PD-L2 are known to inhibit activation of immune responses by inducing T-lymphocyte anergy and apoptosis [42-45]. PD-L1 is expressed on resting B cells, T cells, macrophages and DCs [37]. The expression of PD-L1 is further up-regulated on these cells by various stimulation including anti-IgM, anti-CD40 and LPS for B cells; anti-CD3 for T cells; anti-CD40,

LPS, IFN $\gamma$  and granulocyte macrophage colony stimulating factor (GM-CSF) for macrophages; and anti-CD40, IFN $\gamma$ , GM-CSF, IL-4 and IL-12 for DCs [37]. On the other hand, PD-L2 is rarely expressed on resting cells and hardly induced on B cells and T cells [37]. PD-L2 can be induced on macrophages with IFN $\gamma$  and IL-4, and induced on DCs with anti-CD40, IFN $\gamma$ , GM-CSF, IL-4 and IL-12 [37]. IL-4 induces PD-L2 more strongly than IFN $\gamma$ , while IFN $\gamma$  induces PD-L1 more strongly than IL-4 on macrophages, suggesting that T-helper type 1 and type 2 responses mobilize PD-L1 and PD-L2 differentially [46].

TIM3 belongs to the TIM family of molecules that in mice contains 8 members (TIM-1-8) and in humans contains 3 members (TIM-1,3,4) [47]. TIM3 is a novel transmembrane protein that is expressed on Th1 cells, cytotoxic CD8<sup>+</sup> T cells, regulatory T cells, DCs, macrophages, monocytes, microglia and natural killer (NK) cells in mice and humans [48-56]. TIM3 was first found to be involved in the regulation of Th1 cell-mediated immunity [48-50]. The interaction of TIM3 with its ligand galectin-9 dampens the response of both IFN $\gamma$  producing CD4<sup>+</sup> Th1 and CD8<sup>+</sup> effector T cells, inducing cell death; *in vivo* blockade of this interaction results in exacerbated autoimmunity and abrogation of tolerance in experimental models, thus establishing TIM3 as a negative regulatory molecule of the adaptive immune system [48-52]. As well, TIM3 is able to suppress the nucleic acid-mediated innate immune system through interaction with HMGB1; preventing nucleic acid recruitment into DCs, which is important for antitumor immunogenicity in tumor microenvironments that release nucleic acids from dying tumor cells [53].

BTLA is an immunoglobulin domain-containing glycoprotein with two immunoreceptor tyrosine-based inhibitory motifs, is a third inhibitory molecule of lymphocytes that associates with SHP-1 and SHP-2 [57]. Depending on the BTLA allele, BTLA is known to be expressed by CD4<sup>+</sup> Th1 cells, CD8<sup>+</sup> T cells, B cells, macrophages, DCs, and NK cells [22, 35, 57-59]. BTLA inhibits T cell proliferation and cytokine production *in vitro* and plays a critical role in the induction of peripheral T-cell tolerance *in vivo* [57, 58]. In addition, BTLA mediates the negative regulation of CD8<sup>+</sup> T-cell homeostasis and proliferation *in vivo* [59].

### 1.2.2 Clinical immunotherapies

It is widely believed that blocking these negative regulatory molecules in cancer may attenuate tumor growth. Ipilimumab, a human monoclonal antibody against CTLA4, was approved by the FDA in March 2011 to be used on late stage melanoma [60, 61]. Studies on anti-PD1 antibodies (Nivolumab, Pembrolizumab and Pidilizumab) in various cancers including melanoma have entered stage 2-3 trials since late 2008 [60, 61]. Currently, no clinical studies are currently being conducted on TIM3 or BTLA antibodies against any cancer. Interestingly, some immunotherapies are being tested that block the PD1 ligand on the tumor cell, which has the benefit of potentiating the antitumor response at a tumor-specific level [61]. Ultimately, research on blockade of the PD1/PD-L1 axis holds much promise, with greater response rates and lower toxicity due to their tumor-specific mode of activation, rather than generalized suppression of T cell inhibition [62]. A review on the 3 anti-PD1 and 4 anti-PD-L1 antibodies currently in clinical trials shows encouraging responses rates between 20%-50% that have continued responses after treatment and transient low-grade immune-related adverse effects [63].

## 1.3 Epigenetics

Epigenetics can be defined as regulatory changes that modulate gene expression without changing the DNA sequence itself [64]. Modulation can occur by altering chromatin structure through DNA methylation or histone modification, or further downstream by regulating messenger RNA (mRNA) through non-coding RNAs such as microRNAs (miRNAs) [64, 65]. The beautiful aspect between the concept of epigenetics and genetics is that the former may be therapeutically intervened with greater ease [64]. Currently, a few therapies that affect DNA methylation and histone modification have been approved by the FDA: DNA methyltransferase (DNMT) inhibitors such as Decitabine and Vidaza, and histone deacetylase (HDAC) inhibitors such as Vorinostat and Romidepsin [66]. Although these drugs have been approved for acute leukemia and cutaneous T cell lymphoma [66], recent research has found convincing evidence for the role of epigenetics in future treatments of melanoma such as using histone deacetylase inhibitors and IL-2

[67]. Although miRNAs currently may not have as bold of a therapeutic approach as DNMT or HDAC inhibitors, the possibility exists and also extends to diagnostic and prognostic markers.

## 1.4 RNA interference and microRNAs

One potential mechanism by which PD1, TIM3 and BTLA synthesis can be modulated is by the induction of miRNAs. miRNAs are short (approximately 22 nucleotides) RNAs that regulate gene expression by base pairing with the 3' untranslated regions (UTR) of mRNAs resulting in the translational inhibition or mRNA degradation [68]. Lin-4 was the first miRNA discovered in 1993, in the organism *Caenorhabditis elegans* [69, 70] and five years later it was reported that exogenous double stranded RNA can silence genes through a mechanism termed RNA interference (RNAi) [71]. In 1999, the concept of RNAi was further understood when silencing in plants was correlated to small RNAs that match the sequence of the silenced transcript [72]. By 2001, two categories of small RNAs were classified under an RNAi role: miRNAs and siRNAs. miRNAs are known as regulators of endogenous genes and are expressed endogenously, while siRNAs protect our genome by reacting to foreign or invasive nucleic acids and are primarily exogenous in origin [73]. miRNAs do not have perfect complementarity when in the double stranded stem loop or to the mRNA targets, which allows one miRNA to bind several mRNA transcripts. siRNAs are perfectly complementary in their double stranded form and to their single target mRNA, thus resulting in mRNA degradation [74]. Although in rare cases siRNA that are perfectly matched may not utilize endonuclease activity to degrade mRNA, but rather silence in a way similar to miRNAs [74].

Now it is believed that over 1000 miRNAs exist in humans that regulate over 30% of our genome [75]. miRNAs originate from miRNA genes or introns of protein coding genes and are termed pri-miRNAs upon transcription by RNA polymerase II, resulting in capped and polyadenylated transcripts [76]. Pri-miRNAs have a stem loop shape and are processed by an enzyme Droscha, which is an endoribonuclease that cleaves 11 bp from the bottom of the stem leaving a 22 bp stem loop known as pre-miRNA [68]. From here,

Exportin-5 transports the pre-miRNA into the cytoplasm for further processing by Dicer [76]. Dicer cleaves the terminal loop which generates a double stranded RNA that is approximately 22 base pairs in length and has 3' overhangs that are two nucleotides in length [76]. The last step involves separation of the two strands so that one gets incorporated in the RNA-induced silencing complex (RISC) [77]. The miRNA loaded RISC complex is then directed towards the 3' UTR of target mRNAs, thus inducing repression of protein expression through mRNA degradation or translational inhibition [77].

## 1.5 miRNAs reported in melanoma

Over the years, many miRNAs have been linked to melanoma development as either oncogenic or tumor suppressive miRNAs. miR-195, miR-221, miR-222, miR-193b, miR-15b, miR-199a-5p, miR-424, miR-432-5p and the miR-let-7 family act as oncogenic miRNAs [65, 78-83], while miR-205, miR-26a, miR-34a, miR-125b, miR-18b, miR-573 act as tumor suppressive miRNAs [84-89]. Many other miRNAs have been linked to melanoma, but this list demonstrates the potential for miRNAs to be used clinically for detection, progression, prognosis, and therapy [90]. Although miRNAs such as miR-155 and miR-150 are found upregulated in blood samples of patients suffering from chronic lymphocyte leukemia, it is unknown whether these changes are a result of the tumor or immune cells [91]. This highlights the importance of looking at specific tissue and cell types to understanding altered miRNA expression and its suitability for prognostic or therapeutic markers. As well, some miRNAs may be oncogenic or tumor suppressive depending on the cancer, such as miR-155 [92, 93], further demonstrating the need to understand miRNA regulation in specific diseases and cell types.

### 1.5.1 Prognostic potential

Although much work still needs to be done on prognostic markers in melanoma, summaries can be seen that highlight miRNAs miR-150, miR-342-3p, miR-455-3p, miR-

145, miR-155, and miR-497 as predictors of long-term survival of metastatic melanoma [94]. Another study looked at lymph node metastasis and discovered that miR-191 was under-expressed and miR-193b was over-expressed in patients with poor melanoma-specific survival [95]. Other studies do exist that have found correlations between additional miRNAs and how they may affect clinical outcome, thus demonstrating the need for more research to determine which miRNAs have the best clinical impact towards long term survival [84, 96, 97].

### 1.5.2 Therapeutic potential

With the discovery of aberrant miRNA signatures in various diseases states, the idea of using antagomirs or miRNA mimics to restore miRNA function has become an intriguing therapeutic concept [98]. Various *in vitro* and *in vivo* studies have shown that use of miRNA mimics and antagomirs to miR-221, miR-222, miR-182, miR34a, miR-16 and miR-203 may prove beneficial in the treatment of advanced melanoma [79, 99-101]. Some issues that arise with the use of miRNA as a direct therapy involves targeted delivery methods, off-target miRNA binding effects and miRNA half-life. Although these issues may prevent the progression of miRNA as direct therapies, the possibility definitely exists that miRNAs can be used to predict response to various therapies. For example, Kheirleif *et al.* used a microarray to identify a group of miRNAs as predictors of response to neoadjuvant chemoradiation therapy [102]. Currently, the expression of PD-L1 using immunohistochemistry (IHC) is used as a predictive biomarker for PD1/PD-L1 therapy [63], however no miRNA biomarkers have been reported. By discovering miRNA biomarkers for use with IHC that can accurately predict therapy response, we can reduce the cost of cancer treatment by increasing objective response rates and minimizing the number of cancer patients that need multiple treatments.

## 1.6 microRNAs in T cell exhaustion

Overall, little experimental research has been conducted on PD1, TIM3 and BTLA synergistically in cancer [31-33, 35], and no experimental research has been done to observe the effects of miRNAs on PD1, TIM3 and BTLA in melanoma and T cell exhaustion. Therefore, this study will provide valuable epigenetic data on the immunoinhibitory target, PD1, which supports the use of miRNAs as prognostic markers and therapeutic molecules to confer T cell immunity against melanoma.

## 1.7 Rationale

Currently, the immunotherapy using Ipilimumab is recommended at 4 cycles of 3 mg/kg per dose given every 3 weeks, which costs approximately \$120,000 [103]. This large cost is a major hurdle for the use of new immunotherapies. It may inhibit the use of new therapies that seek to combine antibodies against the PD1 and CTLA4 pathway that are currently in clinical trials [63], as well, as any other combination of immunotherapy and cancer targeting antibody. By understanding altered miRNA expression in PD1<sup>+</sup> T cells I hope to, for the first time, discover miRNAs that may target PD1 and have potential to be used as a synergistic therapy against multiple immunoinhibitory receptors.

## 1.8 Hypothesis

I hypothesize that miRNAs exist that can silence PD1 and potentially other inhibitory immunoreceptors such as TIM3 and BTLA. As well, that miRNA mimics *in vitro* can act therapeutically to revert symptoms of T cell exhaustion.



## 1.9 Specific aims

The following 4 specific aims were chosen to test my hypothesis:

1. To discover altered miRNA expression between PD1<sup>+</sup> and PD1<sup>-</sup> T cells in melanoma-bearing mice
2. To determine the PD1 silencing ability of candidate miRNAs using miRNA mimics and inhibitors
3. To discover if the silencing candidate miRNAs affect CD4<sup>+</sup> T cell proliferation and apoptosis *in vitro*.

## Chapter 2

### 2 Materials and methods

#### 2.1 B16F10 cell culture

To investigate the miRNA regulation of PD1 in T cells in the context of melanoma, B16F10 mouse melanoma cells were used. B16F10 cells were obtained from ATCC (Manassas, VA). Cells were cultured using DMEM medium (Gibco, Life Technologies, Burlington, ON) made complete with 10% fetal bovine serum (FBS; Gibco), 100 units/mL of penicillin (Gibco) and 100 µg/mL of streptomycin (Gibco) at 37 °C in 5% CO<sub>2</sub>. B16F10 cells were cultured and passaged in tissue culture flasks for at least 4 passages, and were grown to approximately 80% confluency before each experiment was performed.

#### 2.2 Melanoma mouse model

8-10 week old C57BL/6 mice (Charles River Canada, Saint-Constant, Canada) were used to generate a melanoma mouse model. Animals were housed under conventional conditions at the Animal Care Facility, Western University, and were cared for in accordance with the guidelines established by the Canadian Council on Animal Care. Tumors were generated on the backs of each mouse through subcutaneous injection of  $4 \times 10^5$  B16F10 cells in phosphate buffered saline (PBS; Gibco). Tumors were allowed to grow for 16 days or until reaching a size of 2,000 mm<sup>3</sup>. Mice were monitored daily and sacrificed using CO<sub>2</sub> in accordance with the guidelines established by the Canadian Council on Animal Care.

## 2.3 Lymphocyte isolation

### 2.3.1 Lymphocyte isolation from lymph nodes

Lymph nodes were obtained from wild-type (WT) and tumor-bearing mice. Single cell suspensions were generated by pressing lymph nodes through a 40  $\mu$ m Falcon Cell Strainer (VWR, Mississauga, ON) into RPMI 1640 medium (Gibco), and cells were counted and centrifuged for 5 minutes at 1,500 rpm and 4 °C. Depending on the experiment, cells were resuspended in: PBS with 2% FBS; Complete RPMI 1640 medium, made complete with 10% FBS and 500 units of penicillin and 500  $\mu$ g of streptomycin; or Transfection RPMI 1640, composed of 10% FBS and 50mM 2-mercaptoethanol (2-ME; Gibco)

### 2.3.2 Lymphocyte isolation from spleen

Spleens were obtained from WT and tumor-bearing mice. Each spleen was pressed through a 40  $\mu$ m Falcon Cell Strainer into RPMI 1640 medium. The cells were loaded onto 5 mL of Ficoll-Paque (Fisher Scientific, Ottawa, ON) and centrifuged for 25 minutes at 2300 rpm and 20 °C with low acceleration and no deceleration. The middle lymphocyte layer was transferred and resuspended into a fresh tube of RPMI 1640. Cells were counted and centrifuged for 5 minutes at 1,500 rpm and 4 °C. Finally, the cells were resuspended in PBS with 2% FBS.

### 2.3.3 Lymphocyte isolation from tumor tissue

Tumor tissue was obtained from B16F10 tumor-bearing C57BL/6 mice. The tumor tissue was digested in Collagenase IV (Life Technologies) for 30 minutes at 37 °C, while being vortexed every 10 minutes, and then was pressed through a 40  $\mu$ m Falcon Cell Strainer into RPMI 1640 medium. Cells were stained with antibodies from the Pan T Cell Isolation Kit II (Miltenyi Biotec, MA, USA) as per the manufacturer's instruction and run through a magnetic MACS column to isolate unstained T cells. Cells were counted and

centrifuged for 5 minutes at 1,500 rpm and 4 °C before resuspension in PBS with 2% FBS.

## 2.4 Flow cytometry and cell sorting

Flow cytometry was performed using a BD LSR II (BD Biosciences, Mississauga, ON) and cell sorting with a BD FACS Aria III (BD Biosciences, Mississauga, ON). One million cells were suspended in 100 µL of PBS with 2% FBS and stained with 0.2 µg of CD3-FITC, CD4-FITC, CD8-FITC, PD1-PerCP-eFluor 710, TIM3-PE, BTLA-APC, Rat IgG2b Isotype Control-PerCP-eFluor 710, Mouse IgG2a K Isotype Control-PE, Mouse IgG1 K Isotype Control-APC (eBioscience, San Diego, CA) or 0.1 µg of Fixable Viability Dye eFluor 506 (eBioscience) for 30 minutes at 4 °C. Cells were washed with 2 mL of PBS with 2% FBS, centrifuged for 5 minutes at 1,500 rpm and 4 °C, and resuspended in the same medium before flow cytometric analysis and sorting.

## 2.5 miRNA extraction and cDNA synthesis

The miRNeasy Mini Kit (Qiagen, Toronto, ON) was used to isolate total RNA including miRNAs. 700 µL of QIAzol Lysis Reagent was added to lymphocyte cell pellets and homogenized by vortexing. After 5 minutes of incubation at room temperature, 140 µL of chloroform was added and the tube was shaken vigorously for 15 seconds and incubated at room temperature for 3 minutes. The mixture was centrifuged at 12,000 x g for 15 minutes at 4 °C. The upper aqueous phase was transferred to a new tube and mixed with 1.5 times the volume of 100% ethanol. 700 µL of the mixture was filtered through an RNeasy Mini Column at 12,000 x g for 15 second, discarding the flow through. 700 µL of Buffer RWT, and two washes of 500 µL of Buffer RPE were filtered through the column with centrifugation. 50 µL of RNase free water was used to elute the total RNA with centrifugation at 12,000 x g for 2 minutes. RNA concentration was measured using a NanoDrop ND-1000 (Thermo Scientific, Ottawa, ON).

200 ng of total RNA was used with the miScript II Reverse Transcriptase Kit (Qiagen). In 200  $\mu$ L tubes, RNA and water were combined to 12  $\mu$ L and 4  $\mu$ L of 5x miScript HiSpec Buffer, 2  $\mu$ L of 10x Nucleic Mix and 2  $\mu$ L of Reverse Transcriptase Mix was added for a total volume of 20  $\mu$ L. Tubes were incubated at 37 °C for 60 minutes and then the reverse transcriptase was inactivated with incubation at 95 °C for 5 min. cDNA was placed on ice prior to use in reverse transcription quantitative polymerase chain reaction (RT-qPCR).

## 2.6 mRNA extraction and cDNA synthesis

Total RNA was extracted from cells using 0.5 mL of Trizol reagent (Invitrogen, Burlington, ON). 250  $\mu$ L of chloroform was added and mixed vigorously, and the mixture was incubated for 5 min at room temperature before centrifugation at 12,000 x g for 15 minutes at 4 °C. The aqueous layer was removed, mixed with 0.5 mL isopropanol and mixed vigorously before incubation for 10 minutes at room temperature. A pellet was formed after centrifugation at 12,000 x g for 10 minutes at 4 °C and washed with 0.5 mL of 75% ethanol. After washing, pellets were air dried and resuspended in RNase free water (Life Technologies) and incubated for 10 minutes at 60 °C. RNA concentration was measured using a NanoDrop ND-1000.

2  $\mu$ g of mRNA was used for reverse transcription. First, 15.5  $\mu$ L RNA in RNase free water and 1  $\mu$ L oligo-(dT) (0.5 $\mu$ g/ $\mu$ L) were mixed and incubated at 70 °C for 10 minutes. 2  $\mu$ L of 10x 1<sup>st</sup> strand buffer, 1  $\mu$ L of 10mM (deoxyribonucleotide triphosphates) dNTPs and 0.5  $\mu$ L of reverse transcriptase (100 units) (Invitrogen) were added to the reaction mixture. The tube was incubated at 42 °C for 50 minutes and reverse transcriptase was inactivated at 70 °C for 15 minutes. Finally, cDNA was placed on ice before use in RT-qPCR.

## 2.7 miRNA array analysis

The Affymetrix GeneChip 3.0 miRNA Array (Affymetrix, Santa Clara, CA) was used with the FlashTag Biotin HSR RNA Labeling Kit (Affymetrix). To begin, a poly(A) tail was added to each RNA strand. 500 ng of total RNA containing miRNAs was adjusted to 8  $\mu$ L in nuclease-free water. Next, 2  $\mu$ L of RNA Spike Control Oligos was added and the tube was placed on ice. A master mix was made that consisted of the following reaction mixture per RNA sample: 1.5  $\mu$ L 10X Reaction Buffer, 1.5  $\mu$ L 25 mM  $MnCl_2$ , 1.0  $\mu$ L Diluted ATP Mix and 1.0  $\mu$ L Poly A Polymerase Enzyme. The 5  $\mu$ L of master mix was added to the 10  $\mu$ L RNA/Spike Control tube for a final volume of 15  $\mu$ L. The mixture was spun down in a microfuge and incubated at 37 °C for 15 minutes.

After addition of a poly(A) tail, the RNA was tagged with Biotin-labeled RNA. 4  $\mu$ L of 5X FlashTag Biotin HSR Ligation Mix and 2  $\mu$ L of T4 DNA Ligase was added to each 15  $\mu$ L poly(A) RNA sample. The tube was mixed by pipetting, microcentrifuged and incubated at room temperature for 30 minutes. After, the reaction was stopped by adding 2.5  $\mu$ L HSR Stop Solution and the solution was mixed by pipetting and microcentrifuged. 2  $\mu$ L was removed to confirm quality using the Enzyme Linked Oligosorbent Assay (Affymetrix)

The next step involved hybridizing the biotin-labelled RNA to the miRNA array. The hybridization cocktail was made by mixing the following reagents: 66  $\mu$ L 2X Hybridization Mix, 19.2  $\mu$ L 27.5% Formamide, 12.8  $\mu$ L DMSO, 6.6  $\mu$ L 20X Hybridization Controls, 2.2  $\mu$ L Control Oligo B2 (3 nM) and 3.7  $\mu$ L nuclease-free water for a total volume of 110.5  $\mu$ L. The 110.5  $\mu$ L hybridization cocktail was added into the remaining 21.5  $\mu$ L of biotin-labeled RNA. The final mixture was incubated at 99 °C for 5 minutes, followed by another 5 minute incubation at 45 °C. The 130  $\mu$ L mixture was injected into the Affymetrix GeneChip 3.0 miRNA Array and the arrays were loaded into a preheated Affymetrix Hybridization Oven 645 (Affymetrix) at 48 °C and 60 rpm for 16 hours. A list of probes sequences on the miRNA array for the various miRNAs studied in this project are listed in Table 2.1.

**Table 2.1** Affymetrix GeneChip 3.0 miRNA Array miRNA probe sequences

<b>Mature miRNA</b>	<b>Probe Sequence (5' → 3')</b>
miR-103	TCATAGCCCTGTACAATGCTGCT
miR-107	TGATAGCCCTGTACAATGCTGCT
miR-146a	AACCCATGGAATTCAGTTCTCA
miR-150	CACTGGTACAAGGGTTGGGAGA
miR-151-5p	ACTAGACTGTGAGCTCCTCGA
miR-155	ACCCCTATCACAATTAGCATTA
miR-181a	ACTCACCGACAGCGTTGAATGTT
miR-21	TCAACATCAGTCTGATAAGCTA
miR-23a	GGAAATCCCTGGCAATGTGAT
miR-27a	GCGGAACCTAGCCACTGTGAA
miR-28	CTCAATAGACTGTGAGCTCCTT
miR-30b	AGCTGAGTGTAGGATGTTTACA
miR-378b	TCTTCTGACTCCAAGTCCAG
miR-466c-5p	ATATGTACATGCACACACACATCA
miR-467a	CGCATATACATGCAGGCACTTA
miR-5121	GGAGATGTCTCATCACAAGCT
miR-669a-3p	ATACGTGTGTGTGTATGTTATGT
miR-669a-5p	AGACATGAACATGCACACACAAC
miR-let-7e	AACTATACAACCTCCTACCTCA

After hybridization, the hybridization cocktail was extracted from each array and the array was filled with Array Holding Buffer. After equilibrating to room temperature, the arrays were stained using the Fluidics Station 450 (Affymetrix) with the appropriate fluidics and fluidics script for the array format.

Lastly, after staining and washing the array was scanned using the GeneChip Scanner 3000 and Affymetrix GeneChip Command Console software (Affymetrix). The analysis of miRNA data was performed using the Partek Genomics Suite (Partek, St. Louis, MO).

## 2.8 Real-time quantitative PCR

Primers for RT-qPCR detection of significantly altered miRNAs discovered from the miRNA array are unique in the sense that they extend the cDNA of the miRNA for detection by quantitative PCR. The primer sequences are not available, but a list of their targets is displayed in Table 2.2. Real-time PCR reactions were performed in a Stratagene Mx3000P QPCR System (Agilent Technologies, Lexington, MA) using the miScript SYBR green PCR Kit (Qiagen) and miScript Primer Assay (Qiagen). The reaction mixture contained: 10  $\mu$ L 2x QuantiTect SYBR Green PCR Master Mix, 2  $\mu$ L 10x miScript Universal Primer, 2  $\mu$ L 10x miScript Primer Assay and 6  $\mu$ L of cDNA mix in RNase-free water for a total volume of 20  $\mu$ L. The PCR reaction conditions for miRNA analysis was 95 °C for 15 min, and 94 °C for 15 seconds, 55 °C for 30 seconds and 70 °C for 30 seconds (40 cycles). Each miRNA primer was referenced to Homo sapiens small nucleolar RNA, C/D box 61 (SNORD61) and normalized to PD1<sup>+</sup> cells using the  $2^{-\Delta\Delta C_t}$  as described by Livak and Schmittgen [104].

qPCR detection of GAPDH silencing in T cells using siRNA was analyzed in a Stratagene Mx3000P QPCR System (Agilent Technologies, Lexington, MA) with SYBR Green PCR Master Mix (Life Technologies). The reaction mixture was composed of 10  $\mu$ L of 2x SYBR Green PCR Master Mix, 100 ng of cDNA, 100 nM primers for GAPDH and  $\beta$ -Actin (Table 2.3), and RNase-free water brought up to 20  $\mu$ L. The PCR reaction



**Table 2.2** Target sequences of miRNA primers for real time qPCR analysis

<b>Mature miRNA</b>	<b>miRNA Target Sequence (5' → 3')</b>
miR-103	AGCAGCAUUGUACAGGGCUAUGA
miR-107	AGCAGCAUUGUACAGGGCUAUCA
miR-146a	UGAGAACUGAAUUGCAUGGGUU
miR-150	UCUCCCAACCCUUGUACCAGUG
miR-151-5p	UCGAGGAGCUCACAGUCUAGU
miR-155	UUAAUGCUAAUUGUGAUAGGGGU
miR-181a	AACAUUCAACGCUGUCGGUGAGU
miR-21	UAGCUUAUCAGACUGAUGUUGA
miR-23a	AUCACAUUGCCAGGGAAUUCC
miR-27a	UUCACAGUGGCCUAAGUUCCGC
miR-28	AAGGAGCUCACAGUCUAUUGAG
miR-30b	UGUAAACAUCCUACACUCAGCU
miR-378b	CUGGACUUGGAGUCAGAAGA
miR-466c-5p	UGAUGUGUGUGUGCAUGUACAUAU
miR-467a	UAAGUGCCUGCAUGUAUAUGCG
miR-5121	AGCUUGUGAUGAGACAUCUCC
miR-669a-3p	ACAUAACAUAACACACACACGUAU
miR-669a-5p	AGUUGUGUGUGCAUGUUCAUGUCU
miR-let-7e	UGAGGUAGGAGGUUGUAUAGUU
SNORD61	GCTATGATGAATTTGATTGCATTGA TCGTCTGACATGATAATGTATTTTT GTCCTCTAAGAAGTTCTGAGCTT

**Table 2.3** Primers used in RT-qPCR detection of mRNA levels

<b>Mature miRNA</b>	<b>miRNA Target Sequence (5' → 3')</b>
GAPDH Forward	TGATGACATCAAGAAGGTGGTGAA
GAPDH Reverse	TCCTTGGAGGCCATGTAGGCCAT
B-Actin Forward	AGGGAAATCGTGCGTGACATCAAA
B-Actin Reverse	ACTCATCGTACTCCTGCTTGCTGA

conditions were: 95°C for 10 minutes followed by 40 cycles at 95°C for 30 seconds, 58°C for 1 minute and 72°C for 30 seconds. Relative GAPDH gene expression was calculated with  $2^{-\Delta\Delta C_t}$  using  $\beta$ -Actin as a reference gene.

## 2.9 *In silico* analysis

*In silico* analysis was performed by accessing multiple miRNA databases: miRanda, TargetScan Mouse 6.2 and PicTar. In each database, miRNAs were searched that had complementarity to the 3' UTRs of PD1, TIM3 and BTLA. Only miRNAs that were 7mer or 8mer were considered. There are 2 types of 7mer and 1 type of 8mer binding: 7mer-m8 and 8mer miRNAs bind in positions 2-8 of the seed region and 7mer-1A miRNAs bind in positions 2-7 in the seed region with position 8 bound to an A on the mRNA.

## 2.10 pmirGLO dual luciferase plasmid

### 2.10.1 PD1 3' UTR amplification

The 3' UTR of PD1 was amplified using PCR. cDNA from WT C57BL/6 lymphocytes were used in a reaction mixture that contained: 19.8  $\mu$ L nuclease free water, 2.5  $\mu$ L 10x PCR buffer, 0.5  $\mu$ L of 10  $\mu$ M forward and reverse primer (Table 2.4), 0.5  $\mu$ L 10 mM dNTPs, 0.2  $\mu$ L of 5U/  $\mu$ L Taq polymerase (Invitrogen) and 1  $\mu$ L cDNA. Sample was thermocycled at 94 °C for 3 minutes, and run through 40 cycles at 94 °C for 30 seconds, 58 °C for 30 seconds and 72 °C for 30 seconds before a final incubation at 72 °C for 10 minutes.

The amplified cDNA was run on a 1.5% agarose gel and the QIAquick Gel Extraction Kit (Qiagen) was used to isolate the DNA from reaction mixture components. The DNA fragment was excised from the agarose gel and 3 volumes of buffer QG was added to 1 volume of gel (100 mg ~ 100  $\mu$ L). After a 10 minute incubation at 50 °C, 1 gel

**Table 2.4** PD1 3' UTR primer sequences

<b>Primer Name</b>	<b>Primer Sequence (5' → 3')</b>
PD1 3' UTR Forward	ATATACTCGAGCCAGATTCTTCAGCCATTAGCATG CT
PD1 3' UTR Reverse	GCGTGTCTAGATTTAAAGCTTTTGGTACCATTTAA TTATAACGGGCT

volume of isopropanol was added to the sample and mixed by inverting the tube. The sample was applied to a QIAquick column and centrifuged for 1 minute at 12,000 x g. The flow through was discarded and two washes were done using 500 µL of buffer QG1 and then 750 µL of buffer PE followed by centrifugation for 1 minute at 12,000 x g for each wash. The QIAquick column was placed in a new Eppendorf tube and 50 µL of buffer EB was added onto the membrane to elute the DNA.

### 2.10.2 Restriction enzyme digestion and ligation

500 ng of amplified PD1 3' UTR and pmirGLO Dual Luciferase Plasmid were cut with XhoI and XbaI restriction enzymes (New England Biolabs, Ipswich, MA). The plasmid and PD1 3' UTR were cut in separate tubes that contained both restriction enzymes. 12 units of each restriction enzyme were used in a total volume of 28 µL consisting of 10x buffer and nuclease free water. The reaction mixture was incubated at 37 °C for 30 minutes. 50 ng of cut plasmid and 35 ng of cut insert were ligated overnight at 16 °C. The ligation used a 5:1 molar ratio of insert:vector and a T4 DNA ligase (New England Biolabs), in a total volume of 20 µL.

### 2.10.3 Amplification and sequencing

The PD1 3' UTR pmirGLO Dual Luciferase Plasmid was amplified in JM109 cells (Promega, Madison, WI). First, JM109 cells were thawed on ice for 5 minutes and mixed before transferring 50 µL to a chilled sterile polypropylene culture tube. 25 ng of PD1 3' UTR pmirGLO plasmid was added to the competent cells and placed on ice for 10 minutes. Cells were heat-shocked at 42 °C for 45 seconds, placed on ice for 2 minutes, added to 450 µL of lysogeny broth (LB; Life Technologies) containing 100µg/mL ampicillin (Bioshop, Richmond, BC) and were shaken at 37 C° for 60 minutes. All 500 µL was plated on ampicillin containing LB plates overnight, and afterwards clones were isolated and shaken overnight at 37°C in 5 mL of LB broth containing ampicillin. Plasmid was extracted using the GeneJET Plasmid Miniprep Kit (Fermentas, Burlington,

ON). Cells were pelleted in a centrifuge and resuspended in 250  $\mu$ L of resuspension solution. 250  $\mu$ L of lysis solution was added and mixed by inverting the tube, and then 350  $\mu$ L of neutralization solution was added and mixed by inverting the tube. Cells were centrifuged for 5 minutes at 12,000 x g. The supernatant was transferred to a GeneJET spin column and centrifuged for 1 minute at 12,000 x g. The flow through was discarded and two washes of 500  $\mu$ L wash solution was added and the column centrifuged for 1 minute at 12,000 x g each time. The plasmid was eluted from the column by adding 50  $\mu$ L of elution buffer, waiting 2 minutes and centrifuging the columns at 12,000 x g for 2 minutes. The concentration of the plasmid was then measured using a NanoDrop ND-1000.

Sequencing was done using the BigDye Terminator v3.1 Cycle Sequencing Kit (Applied Biosystems, Foster City, CA). Initially, 1.5  $\mu$ g of PD1 3' UTR pmirGLO plasmid was brought up to a final volume of 20  $\mu$ L in nuclease-free water after the following reaction conditions were added: 8  $\mu$ L Terminator Ready Reaction Mix and 2  $\mu$ L of 2 $\mu$ M PD1 3' UTR forward primer (Table 2.4). The sample was mixed briefly, and spun down before cycle sequencing was performing on a GeneAmp PCR System 9600 (Applied Biosystems). Tubes were heated to 95 °C for 5 minutes and then cycled 50 times at 95 °C for 30 seconds, 55 °C for 10 seconds and 60 °C for 4 minutes. Tubes were cooled down to 4 °C before purification of extension products using the Performa DTR V3 96-Well Short Plate Kit (Edge Biosystems, Gaithersburg, MD). Lastly, sequencing of purified extension product was performed in an Applied Biosystems 3730 DNA Analyzer.

#### 2.10.4 Plasmid and miRNA mimic transfection

The list of miRNA mimics (Qiagen) transfected with the PD1 3' UTR pmirGLO plasmid are shown in Table 2.5. 60,000 B16F10 cells per well were plated overnight before transfection in 24 well plates using culture medium. On the day of transfection, cells were washed with PBS and 300  $\mu$ L of Opti-MEM was added. In an Eppendorf tube, 0.2  $\mu$ g of

**Table 2.5** miRNA mimic sequences / miRNA inhibitor targets

<b>miRNA mimic</b>	<b>miRNA sequence (5' → 3')</b>
miR-28	AAGGAGCUCACAGUCUAUUGAG
miR-150	UCUCCCAACCCUUGUACCAGUG
miR-103	AGCAGCAUUGUACAGGGCUAUGA
miR-107	AGCAGCAUUGUACAGGGCUAUC
mimic control	The AllStars Negative Control siRNA sequence is not available, but it has no homology to any known mammalian gene (Qiagen #SI03650318)
inhibitor control	The miRNA inhibitor control sequence is not available, but it is designed to target the AllStars Negative Control siRNA and has no homology to any known mammalian gene (Qiagen #1027271)

plasmid and 1  $\mu\text{g}$  of miRNA mimic were added to 100  $\mu\text{L}$  of Opti-MEM. In a separate tube, 100  $\mu\text{L}$  of Opti-MEM was mixed with 2.4  $\mu\text{L}$  of Lipofectamine 2000 Transfection Reagent (Life Technologies) in a 1:2 ratio of miRNA + plasmid ( $\mu\text{g}$ ):Lipofectamine 2000 ( $\mu\text{L}$ ). After 5 minutes of room temperature incubation, both tubes were mixed and allowed to incubate for 20 minutes at room temperature. Then the 200  $\mu\text{L}$  mixture of Opti-MEM, miRNA mimic and dual luciferase plasmid was added into each well of plated B16F10 cells. After 4 hours incubating at 37 °C and 5%  $\text{CO}_2$ , the wells were topped off with culture medium with 20% FBS and placed back at 37 °C and 5%  $\text{CO}_2$  for 24 hours before analysis in a Lumat LB 9507 luminometer (Berthold Technologies, Oak Ridge, TN).

#### 2.10.5 Dual Luciferase Assay

The Dual-Luciferase Reporter Assay System (Promega) was used to detect firefly and renilla luciferase from the PD1 3' UTR pmirGLO plasmid. 24 hours after transfection with plasmid and miRNA mimic, B16F10 cells were washed with PBS in preparation for lysis. Cells were no more than 95% confluent at the time of lysis. 100  $\mu\text{L}$  of passive lysis buffer was added to each well and the plate was rocked gently for 15 minutes. The lysate was transferred to an Eppendorf tube for detection in a Lumat LB 9507 luminometer (Berthold Technologies). 100  $\mu\text{L}$  of Luciferase Assay Reagent II was predispensed in polypropylene tubes and 20  $\mu\text{L}$  of cell lysate was added and mixed by pipetting. After a 10 second measurement for firefly luciferase activity, 100  $\mu\text{L}$  of Stop & Glo reagent was added and the tube was vortexed. The sample was placed back in the luminometer and renilla luciferase activity was measured for 10 seconds. Each sample was read twice, and luciferase activity (firefly luciferase/renilla luciferase) was normalized to the miRNA mimic control and PD1 3' UTR pmirGLO transfection.



## 2.11 Lymphocyte treatment with anti-CD3e and IFN $\gamma$

Lymphocytes isolated from lymph nodes of C57BL/6 mice were treated with anti-CD3e (BD Biosciences) or IFN $\gamma$  (Peprotech, QC) by plating 2 million cells in 24 well plates. For treatment with anti-CD3e, the plates were coated with various concentrations (from 0 – 25  $\mu\text{g/mL}$ ) of anti-CD3e in 200  $\mu\text{L}$  of PBS overnight at 4 °C. Plates were washed with PBS before lymphocytes were plated in Complete RPMI 1640. Treatment with IFN $\gamma$  involved adding various concentrations (0 – 20 ng/mL) to the well at the time of plating. With both treatments, lymphocytes were incubated at 37 °C and 5% CO<sub>2</sub> for 24 hours before cells were collected for flow cytometry.

## 2.12 T cell transfection with siRNA, miRNA mimics and inhibitors

Lymphocytes from the lymph nodes of WT C57BL/6 mice were plated 2 million per well in a 24 well plate using 400  $\mu\text{L}$  of RPMI 1640 with 10% FBS and 50 mM 2-ME (Transfection RPMI 1640 medium). 1  $\mu\text{g}$  of miRNA mimic, miRNA inhibitor (Qiagen) (Table 2.5) or siRNA (Ambion, Austin, TX) (Table 2.6) was added to 50  $\mu\text{L}$  of Opti-MEM and various ratios of transfecting reagent was added to a separate tube with 50  $\mu\text{L}$  of Opti-MEM. A 2:1, 1:1, 1:2, 1:4 and 1:6 ratio of siRNA ( $\mu\text{g}$ ):transfection reagent ( $\mu\text{L}$ ) was used for the initial experiments on T cell transfections and a 2:1 ratio was used for the rest. After 5 minutes of room temperature incubation, the RNA and transfection reagent tubes were combined and incubated for 20 minutes at room temperature. The 100  $\mu\text{L}$  mixture was then added to each well. After 4 hours of incubation at 37 °C and 5% CO<sub>2</sub>, 500  $\mu\text{L}$  of Transfection RPMI 1640 was added to each well and the plates were incubated for up to 48 hours at 37 °C and 5% CO<sub>2</sub> before cells were collected for various experiments.

**Table 2.6** Small interfering RNA sequences

<b>Gene</b>	<b>siRNA sequence (5' → 3')</b>
GAPDH	The Silencer Cy3-labelled GAPDH siRNA sequence is not available (Ambion #AM4649)
control siRNA	The negative control siRNA sequence is not available, but it has no significant homology to any known gene sequences from mice, rats or humans (Ambion #AM4611)

## 2.13 Analysis of proliferation and apoptosis using flow cytometry

For functional analysis of CD4<sup>+</sup> T cells after miRNA mimic transfection, CD4 MACS beads (Miltenyi Biotec) were used to purify CD4<sup>+</sup> T cells before flow cytometric analysis. The cells were stained as per manufacturer's instructions and run through a magnetic column to positively isolate the CD4<sup>+</sup> T cells.

To visualize cell proliferation, lymphocytes were transfected as described in 2.12 and stained with carboxyfluorescein succinimidyl ester (CFSE; eBioscience) prior to plating on anti-CD3e coated plates. After transfection, cells were suspended  $50 \times 10^6$  cells/mL in PBS and CFSE was added to a final concentration of 5  $\mu$ M. Cells were mixed rapidly to evenly disburse the CFSE and incubated at room temperature for 5 minutes. Cells were wash with 10 volumes of PBS containing 5% FBS and centrifuged at 1500 rpm and 20°C for 5 minutes. After 3 washes, the cells were resuspended in Complete RPMI 1640 medium and plated on anti-CD3e coated plates for 4 days before CD4 MACS bead isolation, PD1 PerCP eFluor 710 staining and analysis by flow cytometry. As cells proliferate, the CFSE staining gets split to the daughter cells creating a weaker CFSE signal. Therefore, CFSE<sup>low</sup> signal peaks were gated to quantify the percentage of proliferating cells.

To measure apoptosis, cells were transfected as described in 2.12, and stained with PD1-PerCP-eFluor 710, and Viability Dye eFluor 506 as described in 2.4 after CD4 MACS beads isolation. After PD1 and viability staining, cells were suspended in 100  $\mu$ L of Annexin V Binding Buffer (BD Biosciences) and 5  $\mu$ L of Annexin V-FITC (BD Biosciences) was added. After a 15 minute incubation at room temperature, 200  $\mu$ L of Annexin V Binding Buffer were added and cells were analyzed by flow cytometry. Cells that double stain for eFluor 506 and Annexin V are in late apoptosis, while cells that only stain for Annexin V are in early apoptosis. Viable cells stain double negative.

## 2.14 Statistical analysis

Either a one-way analysis of variance (ANOVA) or a two-tailed unpaired Student's T test was used to determine significance for all experiments. Signification was determined if  $p < 0.05$ . Further details can be found in each figure legend.

## Chapter 3

### 3 Results

#### 3.1 PD1 displays increased expression in T cells isolated from lymphoid and tumor tissue in a B16F10 mouse melanoma model

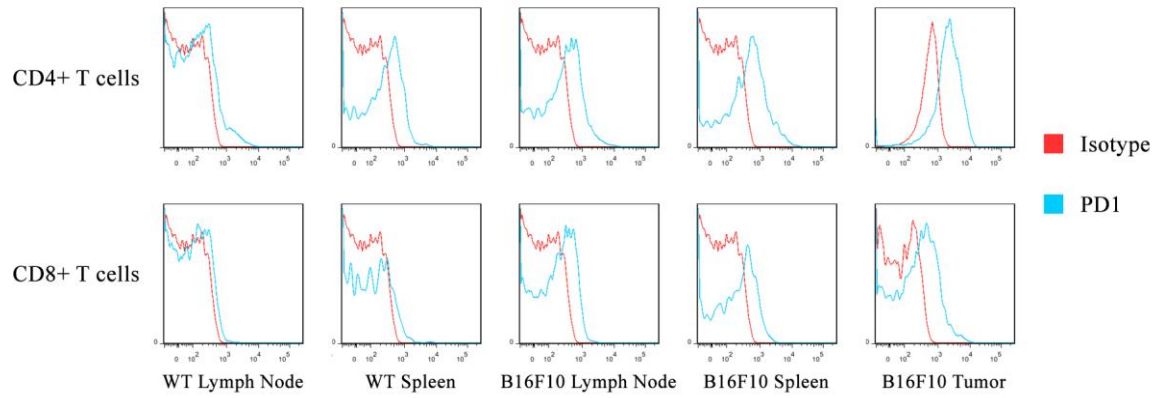
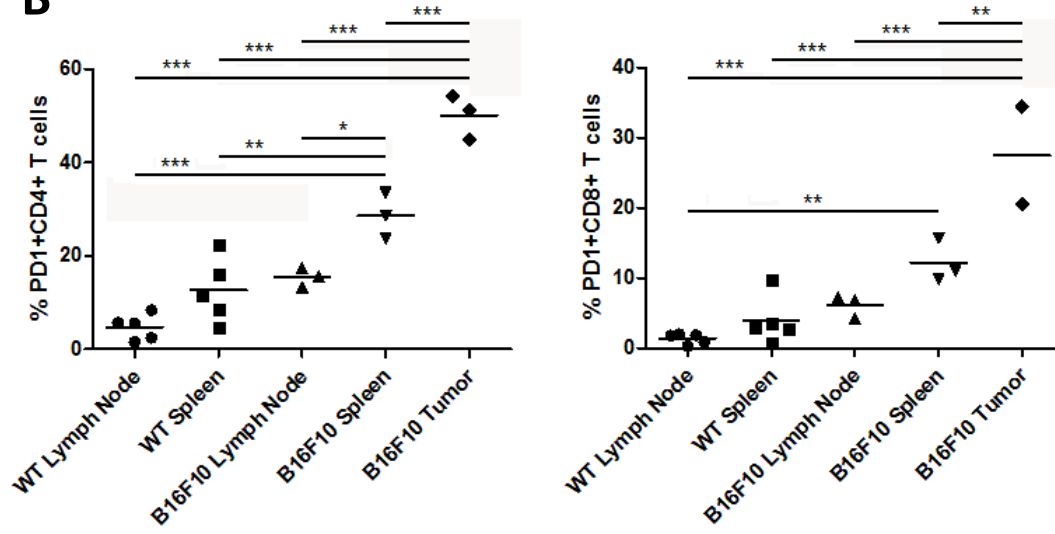
To develop a B16F10 murine melanoma model, C57BL/6 mice were injected with 400,000 B16F10 cells in two spots on their back and tumors were allowed to grow for 16 days before isolating lymphocytes from the lymph nodes, spleen and tumors. Next, flow cytometry was performed to determine the PD1 expression profile in T cell-containing tissues between WT and B16F10 injected mice. PD1 expression was significantly increased in B16F10 tumor-bearing mice compared to WT mice (Figure 3.1A). On CD4<sup>+</sup> T cells, PD1 expression significantly increased in the spleens from B16F10 tumor-bearing mice compared to WT lymph node, WT spleen and B16F10 lymph node (Figure 3.1B). CD8<sup>+</sup> T cells demonstrated a significant increase in B16F10 spleens over WT lymph nodes (Figure 3.1B). In the tumor tissue, CD4<sup>+</sup> T cells displayed 48.1% PD1 expression while CD8<sup>+</sup> T cells displayed 27.45% PD1 expression (Figure 3.1B). Since only approximately 50,000 T cells could be isolated from each tumor, and CD8<sup>+</sup> T cells express PD1 to a lesser extent, it was decided to sort CD4<sup>+</sup> T cells from the lymph nodes and spleen for microRNA array analysis.

#### 3.2 11 miRNAs have altered expression in PD1<sup>+</sup>CD4<sup>+</sup> T cells

To analyze the global miRNA expression profile between PD1<sup>+</sup> and PD1<sup>-</sup> T cells, PD1<sup>+</sup>CD4<sup>+</sup> and PD1<sup>-</sup>CD4<sup>+</sup> T cells were sorted from lymph nodes and spleen using a FACS Aria III and total RNA including miRNA was extracted. 800 ng of RNA was used for the Affymetrix GeneChip 3.0 miRNA array. No significant differences were found between the miRNA expression profiles of either tissue, so data from the both tissues were pooled. A heatmap was generated looking at miRNAs with a fold change of +/- 2,

**Figure 3.1 CD4<sup>+</sup> and CD8<sup>+</sup> T cells from lymph nodes, spleens and tumors of B16F10 tumor-bearing mice express significantly more PD1 than T cells from WT mice.**

CD4<sup>+</sup> and CD8<sup>+</sup> T cells were isolated from the lymph nodes and spleen of WT mice and lymph node, spleen and tumors of B16F10 injected mice. **(A)** PD1 expression on viable T cells was analyzed by flow cytometry. **(B)** A one-way ANOVA followed by a Tukey's post-hoc test was used to compare PD1 expression levels between tissues. Signification was determined if  $p < 0.05$  (\* =  $p < 0.05$ , \*\* =  $p < 0.01$  and \*\*\* =  $p < 0.001$ ). The data shown are representative of at least two independent experiments.

**A****B**

which found 11 significantly downregulated and 8 significantly upregulated miRNAs in PD1<sup>+</sup>CD4<sup>+</sup> T cells (Figure 3.2). In order to confirm the results of miRNA array, 200 ng of RNA was used for real time RT-qPCR analysis on the 19 miRNAs. Figure 3.3 displays discrepancies between the miRNA array and qPCR data, showing that only 3 down regulated miRNAs (miR-150, miR-28 and miR-151-5p) and 8 upregulated miRNAs (miR-let-7e, miR-103, miR-107, miR-27a, miR-23a, miR-21, miR-155 and miR-146a) showed similar trends in altered miRNA expression levels. miR-28, miR-150 and miR-151-5p expression in PD1<sup>+</sup>CD4<sup>+</sup> T cells decreased by 30%, 45% and 25%, respectively (Figure 3.4A) and miR-let-7e, miR-103 and miR-107 increased by 189%, 328% and 318%, respectively (Figure 3.4B). 5 miRNAs; miR-27a, miR-23a, miR-21, miR-155 and miR-146a displayed even greater increases in expression in PD1<sup>+</sup>CD4<sup>+</sup> T cells by 754%, 932%, 993%, 1239% and 2096%, respectively (Figure 3.4C).

### 3.3 *In silico* analysis of miRNAs that may bind to the 3' UTR of PD1, TIM3 and BTLA

To discover miRNAs that may bind to the 3' UTR of PD1, TIM3 and BTLA an *in silico* database search was conducted using miRanda, TargetScan and PicTar. Of note, miR-28 and miR-150 have significant complementarity to all 3 inhibitory immunoreceptors, and miR-103 and miR-107 were complementary to PD1 and BTLA (Table 3.1 and Figure 3.5). Therefore, in accordance with the miRNA array data, these 4 miRNAs were chosen as candidates for further study.

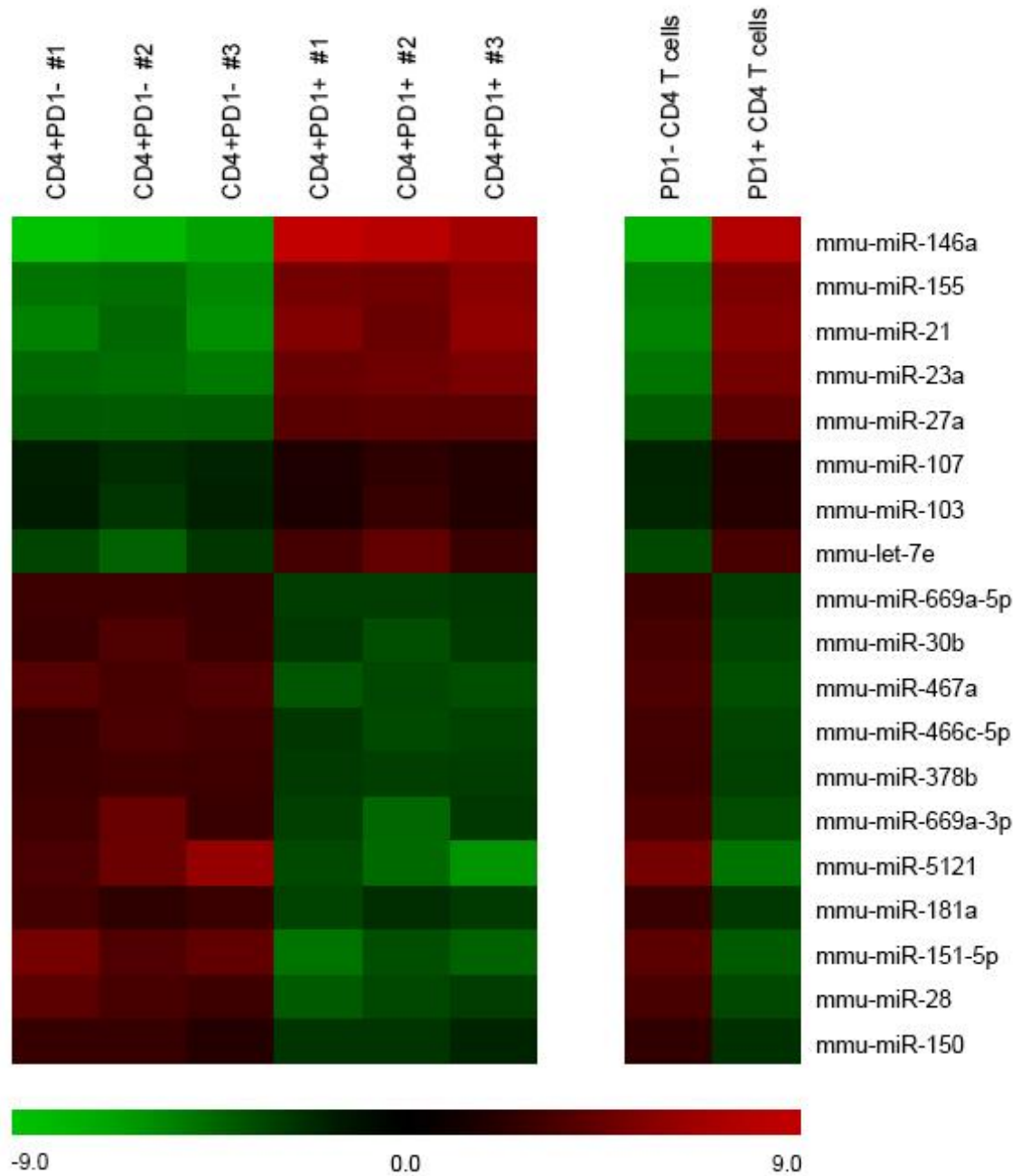
### 3.4 miR-28 and miR-107 silence PD1 through its 3' UTR

To determine whether any of the 4 candidates could silence PD1 through its 3' UTR, a dual luciferase assay was conducted. The 3' UTR of PD1 was amplified from WT C57BL/6 lymph nodes and ligated into the pmirGLO Dual Luciferase miRNA Target Expression Vector (Promega, USA) directly downstream of firefly luciferase. B16F10

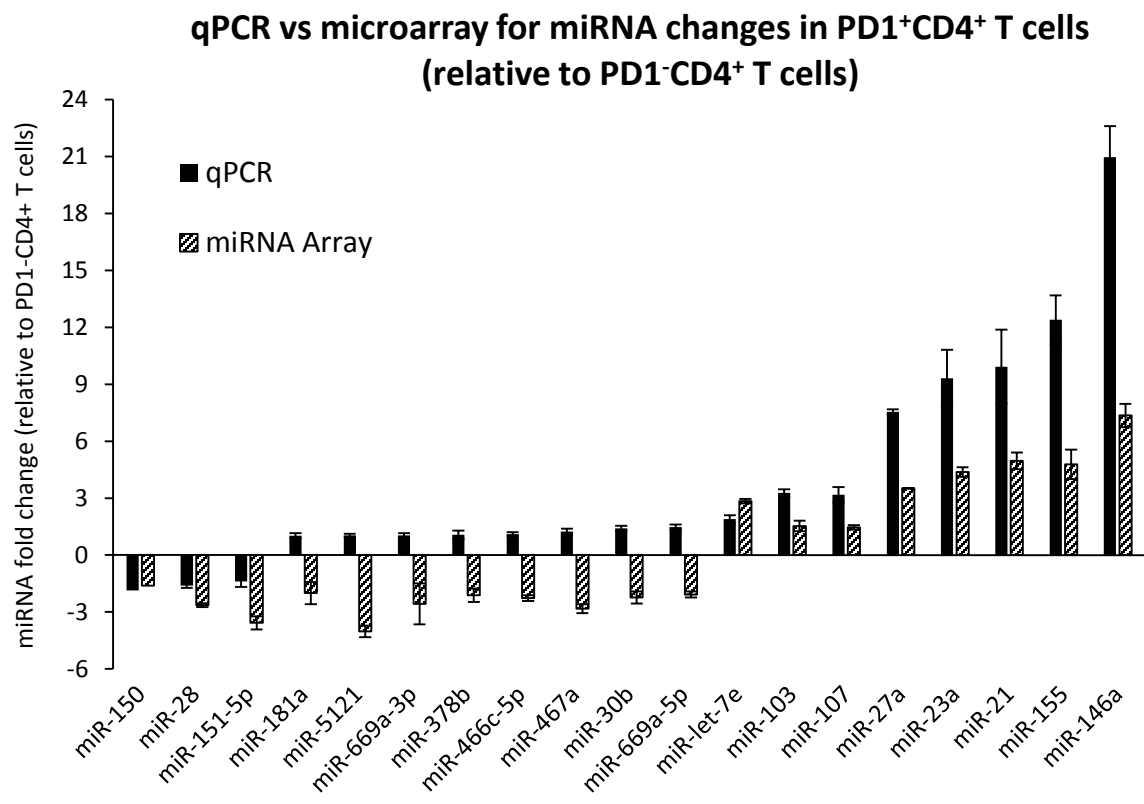


**Figure 3.2 19 miRNAs have significantly altered expression between CD4<sup>+</sup>PD1<sup>-</sup> and CD4<sup>+</sup>PD1<sup>+</sup> T cells isolated from tumor-bearing mice.** Using the Affymetrix GeneChip 3.0 miRNA Array a total of 1,966 mouse miRNAs were analyzed in PD1<sup>+</sup> and PD1<sup>-</sup> CD4<sup>+</sup> T cells. The heat maps represent 19 miRNAs with a fold change greater than +/- 2 between CD4<sup>+</sup>PD1<sup>-</sup> and CD4<sup>+</sup>PD1<sup>+</sup> samples. The left heat map shows fold changes between CD4<sup>+</sup>PD1<sup>-</sup> and CD4<sup>+</sup>PD1<sup>+</sup> T cells from three individual experiments, and the right heat map shows the average fold-change from all samples.

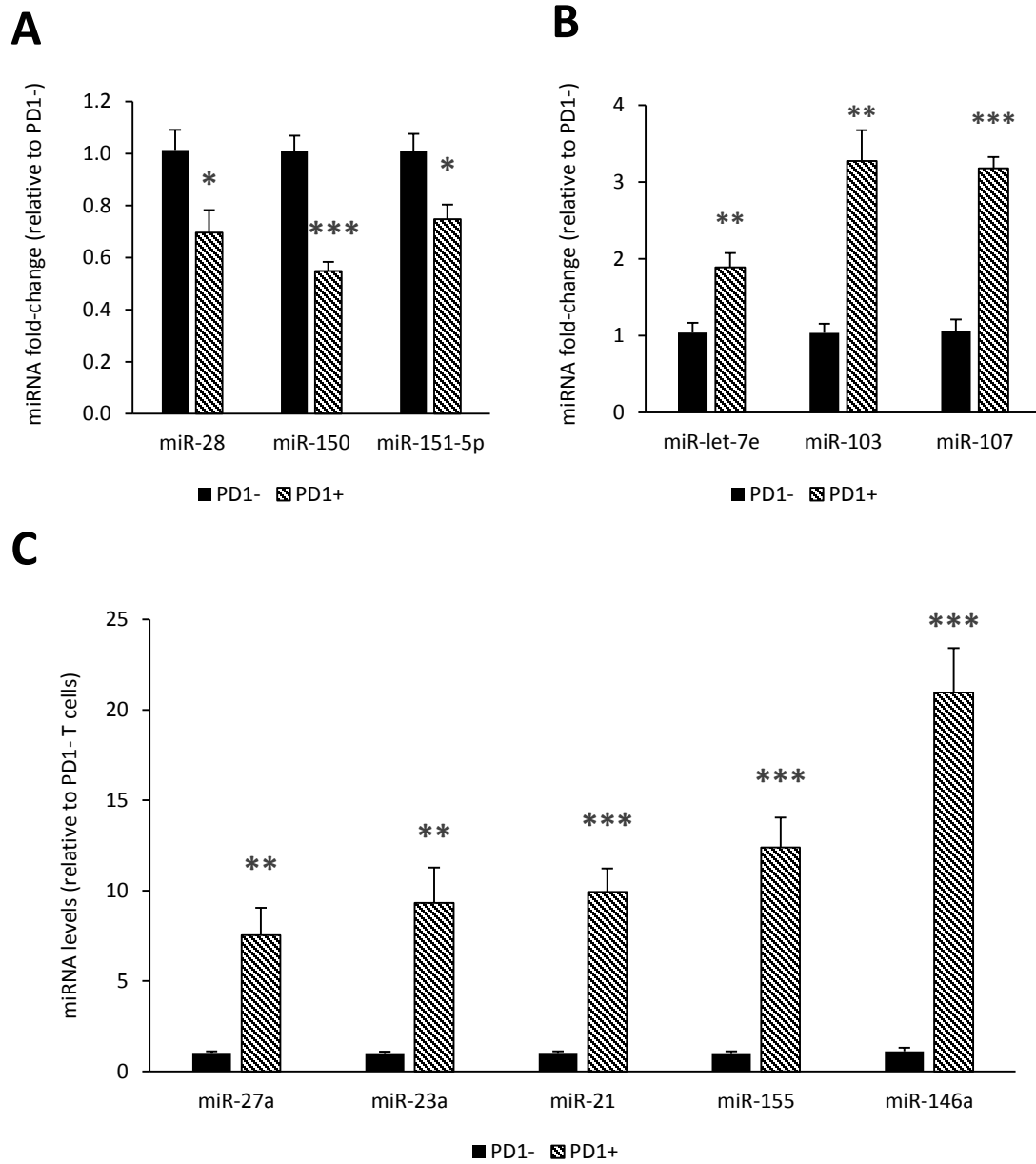
### miRNA array between CD4<sup>+</sup>PD1<sup>+</sup> and CD4<sup>+</sup>PD1<sup>-</sup> T cells



**Figure 3.3 Fold changes in miRNA expression between PD1<sup>+</sup>CD4<sup>+</sup> and PD1<sup>-</sup>CD4<sup>+</sup> T cells determined by the miRNA array and qPCR data.** In order to discover discrepancies between the miRNA array and qPCR data, fold-changes were compared and only the miRNAs with equal trends were considered for further study. The data shown are representative of three independent experiments.



**Figure 3.4 RT-qPCR confirms 11 significantly up- and downregulated miRNAs discovered in the microRNA array.** (A) Significantly downregulated miRNAs in PD1<sup>+</sup>CD4<sup>+</sup> T cells that show an equal trend between the miRNA array and qPCR data. (B-C) Significantly upregulated miRNAs in PD1<sup>+</sup>CD4<sup>+</sup> T cells that show an equal trend between the miRNA array and qPCR data. Significance ( $p < 0.05$ ) between PD1<sup>-</sup> and PD1<sup>+</sup>CD4<sup>+</sup> T cells was determined using an unpaired student's T test (\* =  $p < 0.05$ , \*\* =  $p < 0.01$  and \*\*\* =  $p < 0.001$ ). Data are representative of three independent experiments.

**miRNA changes in PD1<sup>+</sup>CD4<sup>+</sup> T cells (relative to PD1<sup>-</sup>CD4<sup>+</sup> T cells)**

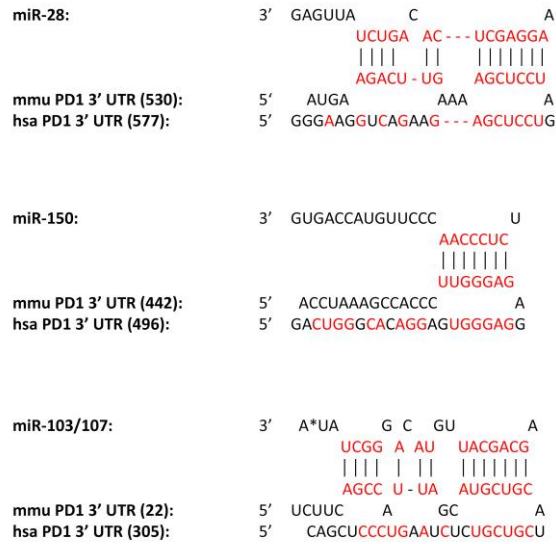
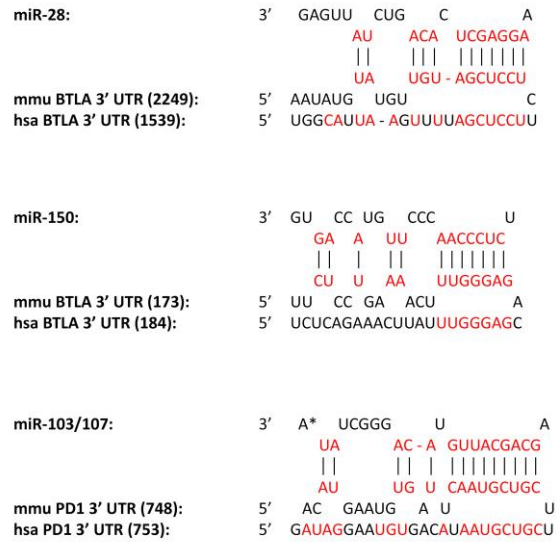
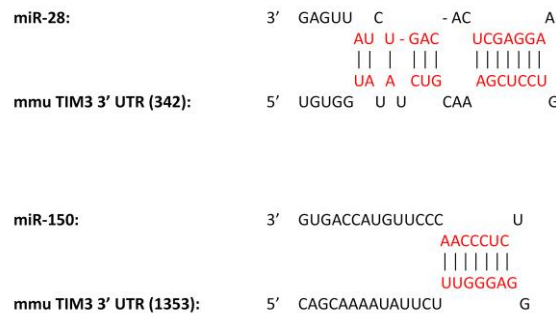
**Table 3.1 miRNA candidates that may silence PD1, TIM3 and BTLA in various combinations.** *In silico* analysis using miRanda, TargetScan and PicTar to discover miRNA candidates that may silence PD1, TIM3 and BTLA in various combinations. The bolded miRNAs represent candidates that were chosen for further study.

**miRNA candidates that may silence PD1, TIM3 and BTLA in various combinations**

<b>PD1 &amp; TIM3</b>	<b>PD1 &amp; BTLA</b>	<b>TIM3 &amp; BTLA</b>	<b>PD1, TIM3 &amp; BTLA</b>
mmu-miR-28	mmu-miR-28	mmu-miR-28	<b>mmu-miR-28</b>
mmu-miR-150	mmu-miR-150	mmu-miR-150	<b>mmu-miR-150</b>
mmu-miR-708	mmu-miR-708	mmu-miR-708	mmu-miR-708
mmu-miR-370	<b>mmu-miR-103</b>	mmu-miR-544	
	<b>mmu-miR-107</b>		
	mmu-miR-154		
	mmu-miR-320		



**Figure 3.5 Candidate miRNA alignment on the 3' UTRs of PD1, BTLA and TIM3 mRNA.** The theoretical bindings sites for miR-28, miR-150 and miR-103/107 on the (A) PD1, (B) BTLA and (C) TIM3 3' UTR. Each miRNA-mRNA combination displays the miRNA, murine 3' UTR and human 3' UTR sequences from top to bottom. Since the sequences for miR-103 and miR-107 differ by only one nucleotide, the \* represents a G and C, respectively. The vertical black lines and red nucleotides represent base-pairing between the miRNA and the murine (mmu) 3' UTR, while the red nucleotides in the human (hsa) 3' UTR are complementary to the miRNA. The number in the bracket denotes the distance in nucleotides from the start of the 3' UTR to the start of the miRNA seed region.

**A****B****C**

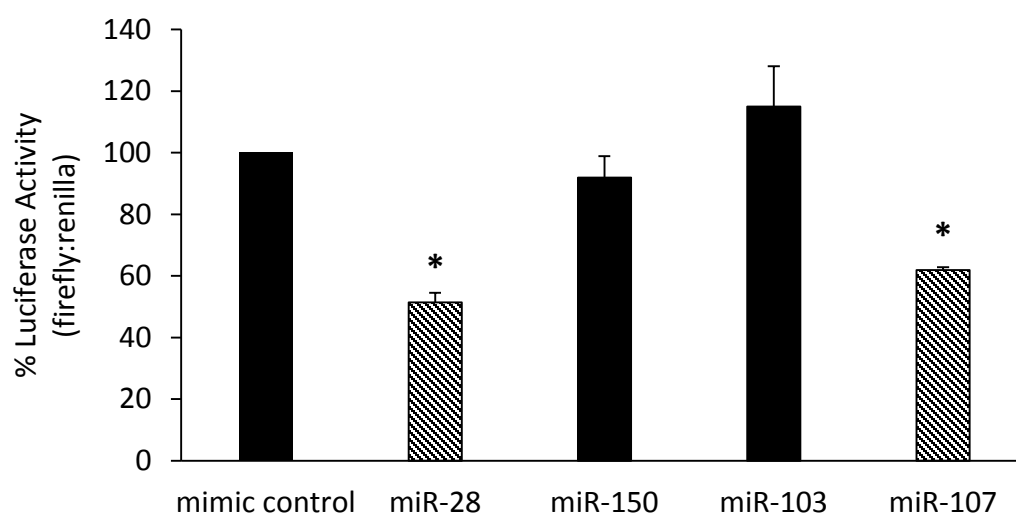
cells were used to transfect the dual luciferase plasmid with miRNA mimics or control miRNA, and 24 hours later cells were collected and analyzed through a luminometer for firefly and renilla luciferase activity. Data showed (Figure 3.6) that miR-28 and miR-107 reduced luciferase activity to 50 and 40%, respectively, while miR-150 and miR-103 had no regulatory effect on the luciferase activity indicating that miR-28 and miR-107 bind to the 3' UTR of the PD1 gene.

### 3.5 Anti-CD3e, but not IFN $\gamma$ , upregulates PD1 and BTLA expression *in vitro*

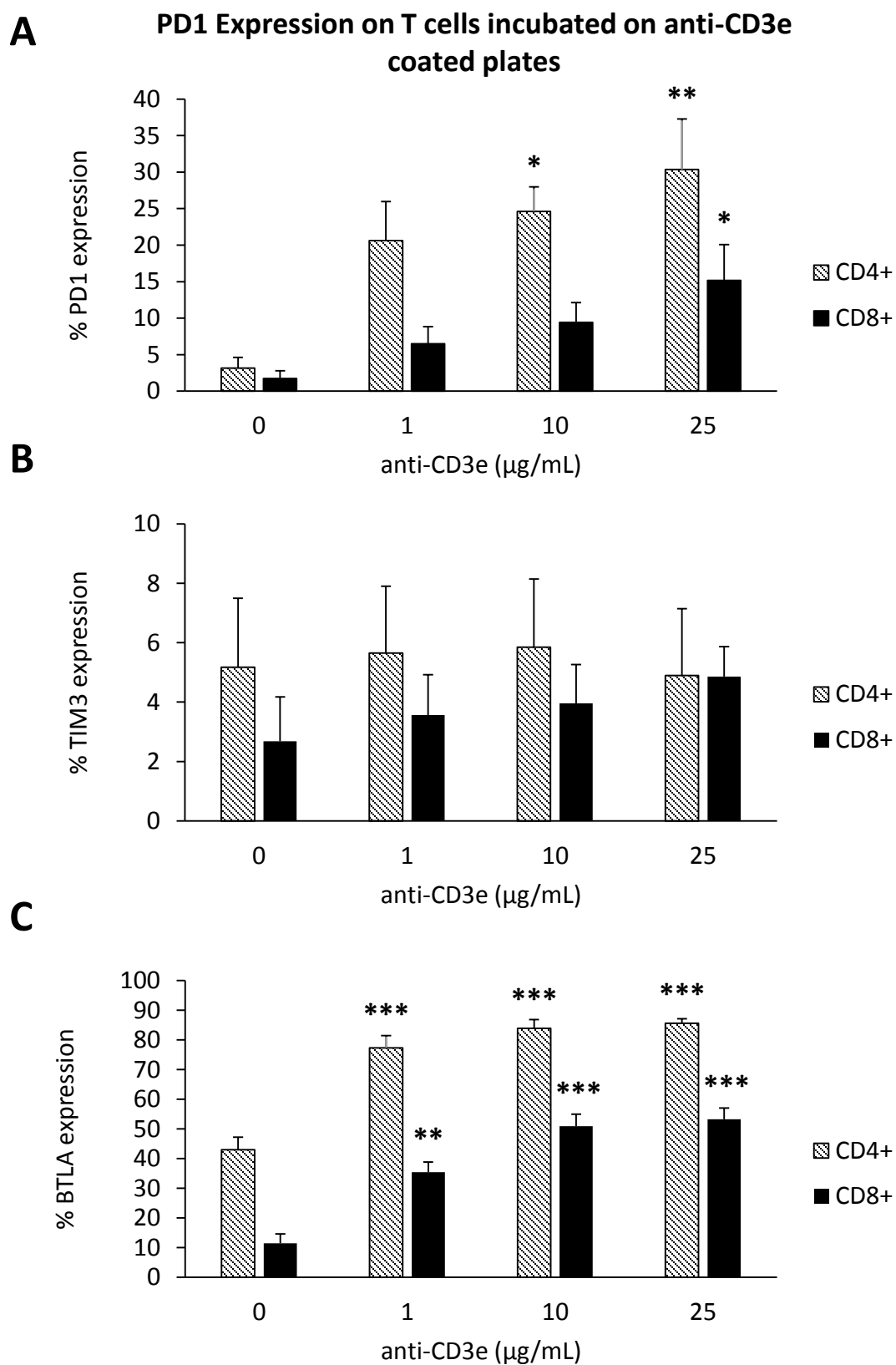
In order to determine if the miRNA expression is altered as a response to PD1 upregulation, rather than a causation, an *in vitro* system needed to be discovered that could upregulate inhibitory immunoreceptor expression. Two methods were attempted, which involved culturing lymphocytes on anti-CD3e coated plates or exposing the cells to IFN $\gamma$ . CD3e stimulation alone, without a CD28 co-activation signal causes the T cell to undergo anergy, a very similar process to T cell exhaustion. As well, previous research has shown that IFN $\gamma$  upregulated PD-L1 expression on human uveal melanoma cells, thus we were curious to discover if IFN $\gamma$  affects PD1 expression on T cells [105]. Initially, 2 million lymphocytes were plated in 24 well plates that were coated with 0, 1, 10 or 25  $\mu\text{g/mL}$  of anti-CD3e overnight or exposed to 0, 1, 5, 10 or 20  $\text{ng/mL}$  of IFN $\gamma$  in the cell culture medium. Cells were cultured for 24 hours and analyzed by flow cytometry. Anti-CD3e treatment significantly increased PD1 and BTLA expression on CD4<sup>+</sup> and CD8<sup>+</sup> T cells in a dose depending manner (Figure 3.7). On the other hand, IFN $\gamma$  had no observable effect on inhibitory immunoreceptor expression (Figure 3.8). Therefore, 10  $\mu\text{g/mL}$  of anti-CD3e was used for subsequent experiments.

**Figure 3.6 miR-28 and miR-107 bind to and silence the PD1 3' UTR.** Dual Luciferase Assay of pmirGLO Plasmid with PD1 3' UTR insert and miRNA mimics. B16F10 cells were transfected with the PD1 3' UTR dual luciferase plasmid and either miRNA mimic or mimic control. Luciferase Activity was measured with a luminometer and normalized to mimic control. A one-way ANOVA followed by a Dunnett's multiple comparison test between miRNA mimic and control was used for statistical analysis, significance was determined if  $p < 0.05$ . The data shown represent three independent experiments.

**Dual Luciferase Assay of miRNA and pmirGLO with  
PD1 3' UTR insert**

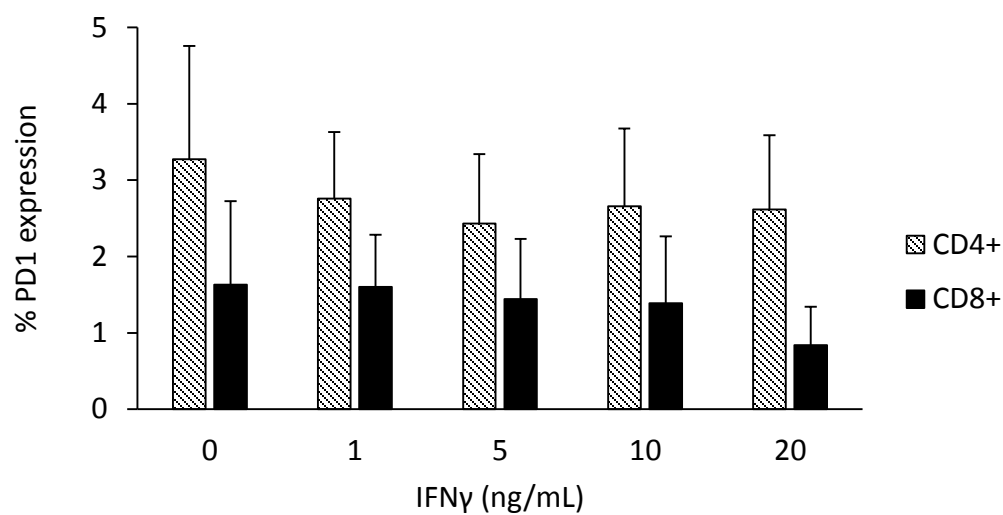
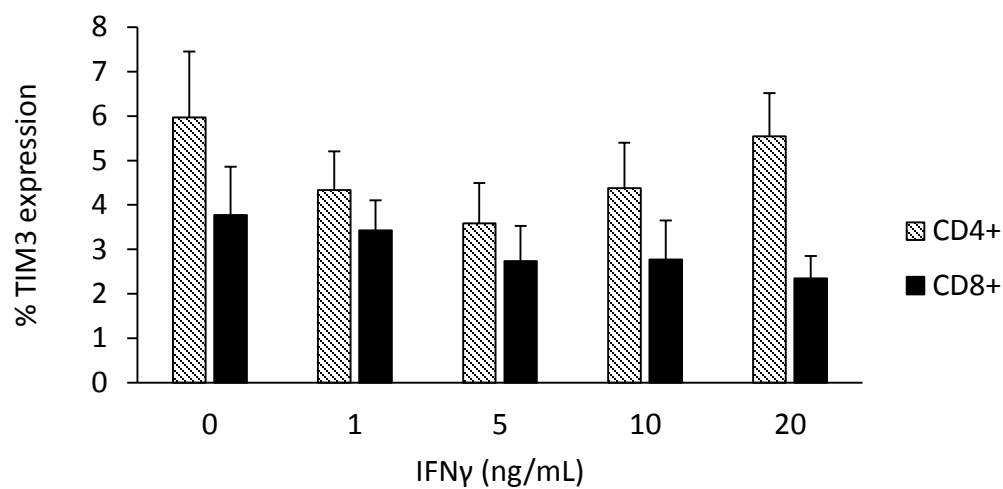
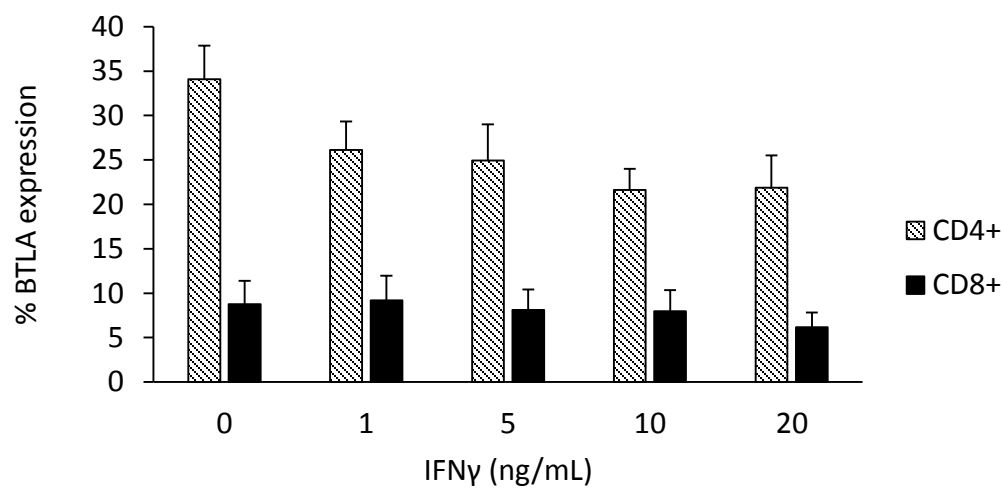


**Figure 3.7 Anti-CD3e treatment increases PD1 and BTLA expression in a dose-dependent manner.** Percent of PD1, TIM3 and BTLA expression on viable CD4<sup>+</sup> or CD8<sup>+</sup> T cells after treatment with various concentrations of anti-CD3e. Lymphocytes were isolated from lymph nodes of WT C57BL/6 mice and 2 million cells/well were plated in a 24-well plate, which was coated with various concentrations of anti-CD3e antibody the night before. 24 hours after plating, cells were stained with Viability Dye eFluor 506, CD4-FITC, CD8-FITC, PD1-PerCP-eFluor 710, TIM3-PE and BTLA-APC, and analyzed by flow cytometry. **(A)** PD1 expression **(B)** TIM3 expression **(C)** BTLA expression. For both T cell subtypes, a one-way ANOVA followed by a Dunnett's multiple comparison test was used to compare immunoreceptor expression alterations between treatment and non-treatment with anti-CD3e. Signification was determined if  $p < 0.05$  (\* =  $p < 0.05$ , \*\* =  $p < 0.01$  and \*\*\* =  $p < 0.001$ ). The data shown are representative of three independent experiments.



**Figure 3.8 IFN $\gamma$  treatment has no effect on PD1, TIM3 or BTLA expression.** Percent of PD1, TIM3 and BTLA expression on viable CD4<sup>+</sup> or CD8<sup>+</sup> T cells after exposure to various concentrations of IFN $\gamma$ . Lymphocytes were isolated from lymph nodes of WT C57BL/6 mice and 2 million cells/well were plated in a 24-well plate. 0, 1, 5, 10 or 20 ng/mL of IFN $\gamma$  was added to the wells and cells were incubated at 37 °C for 24 hours. Flow cytometric analysis was performed after cells were stained with Viability Dye eFluor 506, CD4-FITC, CD8-FITC, PD1-PerCP-eFluor 710, TIM3-PE and BTLA-APC. (A) PD1 expression (B) TIM3 expression (C) BTLA expression. For both T cell subtypes, a one-way ANOVA followed by a Dunnett's multiple comparison test was used to compare immunoreceptor expression alterations between treatment and non-treatment with IFN $\gamma$ . The data shown are representative of three independent experiments.



**A** PD1 Expression on T cells incubated with IFN $\gamma$ **B****C**

### 3.6 miR-28, miR-150, miR-103 and miR-107 show decreased expression after anti-CD3e treatment

To determine if the miRNA levels discovered in CD4<sup>+</sup>PD1<sup>+</sup> T cells from B16F10 tumor-bearing mice were a result of increased PD1 expression, 2 million lymphocytes were plated per well in a 24 well plate coated with anti-CD3e (10 µg/mL). 24 hours later lymphocytes were collected and CD4<sup>+</sup> T cells purified using MACS beads. RNA was isolated and the expression of the 4 candidate miRNAs was measured with RT-qPCR. Expression was normalized to non-stimulated CD4<sup>+</sup> T cells, resulting in a significant down regulation of the 4 candidate miRNAs. miR-28, miR-150, miR-103 and miR-107 were downregulated to 41.3%, 22.2%, 51.9% and 42.8%, respectively (Figure 3.9).

### 3.7 miR-28 and miR-107 inhibitors increase PD1 expression in CD4<sup>+</sup> T cells *in vitro*

The next step was to reevaluate how these miRNAs may effect inhibitory immunoreceptor expression in a more physiologically relevant state, by transfecting T cells. Although my lab focuses on the immune system in cancer, no one has previously attempted to transfect T cells, so the first step was to optimize the protocol to achieve a high transfection efficiency and viability, and then to demonstrate the ability to knockdown a gene. 1 µg of GAPDH-Cy3 siRNA was transfected into 2 million lymphocytes with varying amounts of Lipofectamine 2000 or Lipofectamine RNAiMAX. Figure 3.10 shows a representative histogram for each group, demonstrating that Lipofectamine 2000 had a superior T cell transfection efficiency after 24 hours compared to RNAiMax. Next, the optimal transfection ratio of siRNA (µg):Lipofectamine 2000 (µL) was determined to be 2:1, which achieved a transfection efficiency of 62.7% and total viability of 29.8% 48 hours after transfection (Figure 3.11). To prove that the optimized transfection efficiency resulted in gene knockdown, lymphocytes were transfected with GAPDH siRNA, control siRNA or left alone. 48 hours later, T cells were isolated using Pan T Cell Isolation Kit II MACS beads and RNA was purified for use in

**Figure 3.9 miR-28, miR-150, miR-103 and miR-107 decrease expression after PD1 upregulation mediated by anti-CD3e binding.** Altered miRNA expression in CD4<sup>+</sup> T cells treated with anti-CD3e. Two million lymphocytes were collected from WT C57BL/6 lymph nodes and plated in a 24 well plate coated with 10 µg/mL of anti-CD3e. 24 hours later CD4<sup>+</sup> T cells were isolate using MACS beads and total RNA, including miRNAs, were isolated and used for real time RT-qPCR to determine the changes in miR-28, miR-150, miR-103 and miR-107 expression after PD1 upregulation mediated by anti-CD3e. Significance ( $p < 0.05$ ) was determined using an unpaired student's T test. Data are representative of three independent experiments. \* =  $p < 0.05$ , \*\* =  $p < 0.01$  and \*\*\* =  $p < 0.001$ .

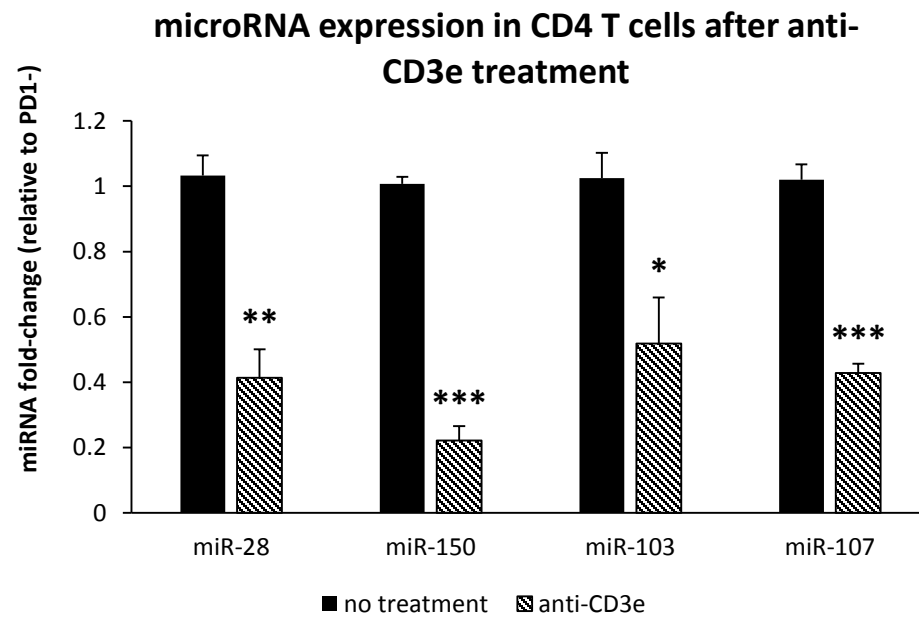


**Figure 3.10 Lipofectamine 2000 demonstrates greater transfection efficiency in T cells compared to Lipofectamine.** 2 million lymphocytes were plated in 24 well plates and 1  $\mu\text{g}$  of GAPDH-Cy3 siRNA was transfected for 24 hours using a 1:2, 1:4, 1:6 or 1:8 ratio of siRNA ( $\mu\text{g}$ ):transfection reagent ( $\mu\text{L}$ ) and transfection efficiency was observed using flow cytometry. Data are displayed as a histogram showing representative efficiency of three independent experiments of GAPDH-Cy3 siRNA transfection into viable  $\text{CD3}^+$  T cells.

Comparison of Lipofectamine 2000 and RNAiMAX on T cell transfection efficiency

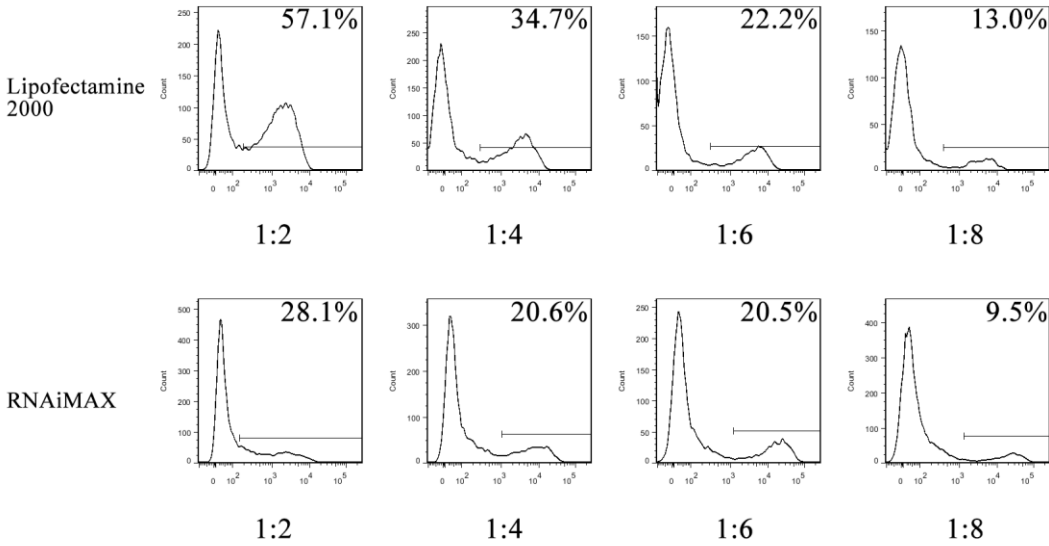
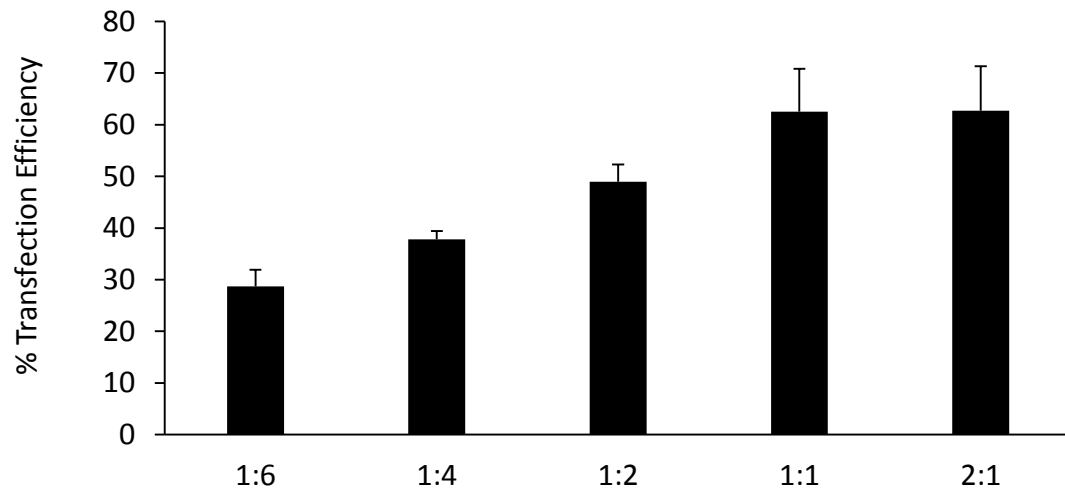
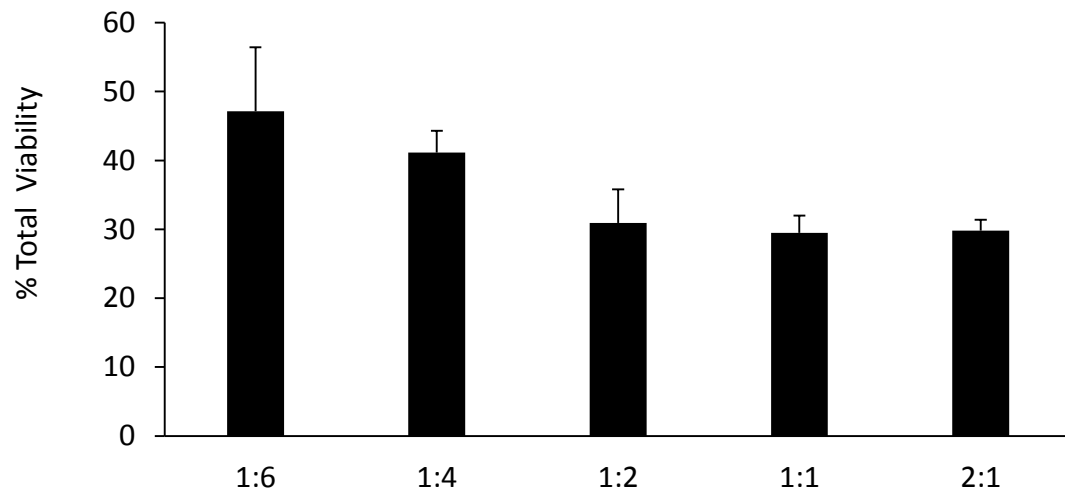


**Figure 3.11 A 2:1 ratio of siRNA ( $\mu\text{g}$ ):Lipofectamine 2000 ( $\mu\text{L}$ ) provides the optimal T cell transfection efficiency and total viability.** 2 million lymphocytes from the lymph nodes of WT C57BL/6 were plated in a 24 well plate and transfected with 1  $\mu\text{g}/\text{mL}$  of GAPDH-Cy3 siRNA while varying the amounts of Lipofectamine 2000. 48 hours after transfection cells were stained with Viability Dye eFluor 506 and CD3-FITC. Flow cytometric analysis was performed to determine the (**A**) transfection efficiency by measuring Cy3 fluorescence in viable CD3<sup>+</sup> T cells and (**B**) total viability by gating on CD3<sup>+</sup> T cells. The data shown are representative of three independent experiments.

**A** Transfection efficiency of Cy3-labelled GAPDH siRNA using varying ratios of siRNA ( $\mu\text{g}$ ):Lipofectamine ( $\mu\text{L}$ )



**B** Total Viability after Cy3-labelled GAPDH siRNA transfection using varying ratios of siRNA ( $\mu\text{g}$ ):Lipofectamine ( $\mu\text{L}$ )





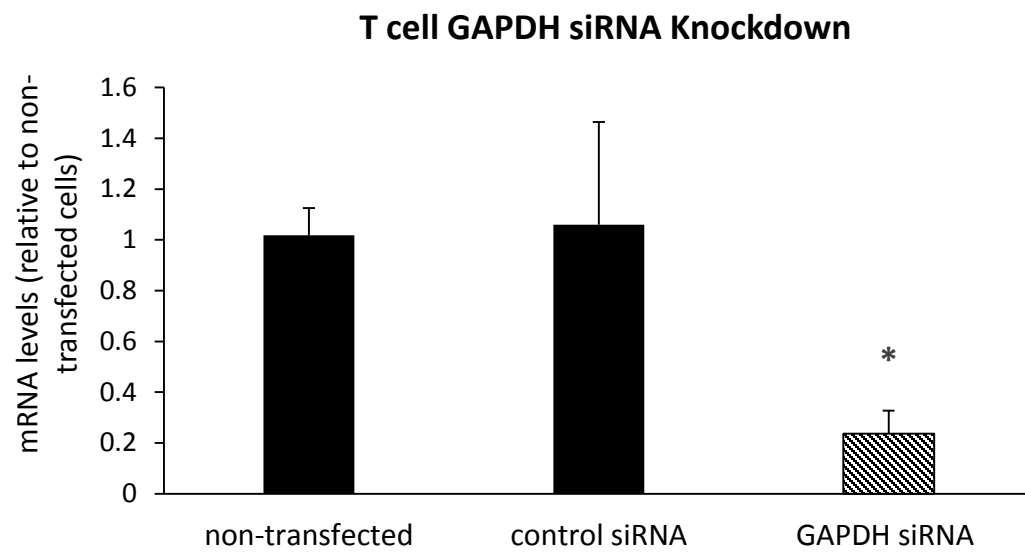
real time RT-qPCR. The data showed that using the GAPDH siRNA, gene expression was silenced approximately 75%, demonstrating the effectiveness of the T cell transfection protocol (Figure 3.12).

Since PD1 expression is low on naïve T cells (Figure 3.1B), a 4 day anti-CD3e treatment was used to induce PD1 expression and to determine if reduction of intrinsic miRNA could increase anti-CD3e stimulated PD1 expression. Two million lymphocytes, collected from the lymph nodes of WT C57BL/6 mice, were plated in a 24 well plate and transfected with miRNA inhibitors for 48 hours using a 2:1 ratio of siRNA:Lipofectamine 2000 ( $\mu\text{g}:\mu\text{L}$ ). After a 4 day exposure to anti-CD3e, cells were collected and stained for PD1, CD4, CD8 and viability. Compared to miRNA inhibitor control, anti-miR-28 and anti-miR-107 transfected CD4<sup>+</sup> T cells demonstrated a 15.66% and 16.39% fold-increase, respectively (Figure 3.13A). CD8<sup>+</sup> T cells displayed a similar trend with 27.38%, 26.15% and 33.77% fold-increase in miR-28, miR-150 and miR-107, respectively (Figure 3.13B). miR-103 transfection had no effect on PD1 expression in both CD4<sup>+</sup> and CD8<sup>+</sup> T cells (Figure 3.13A and B).

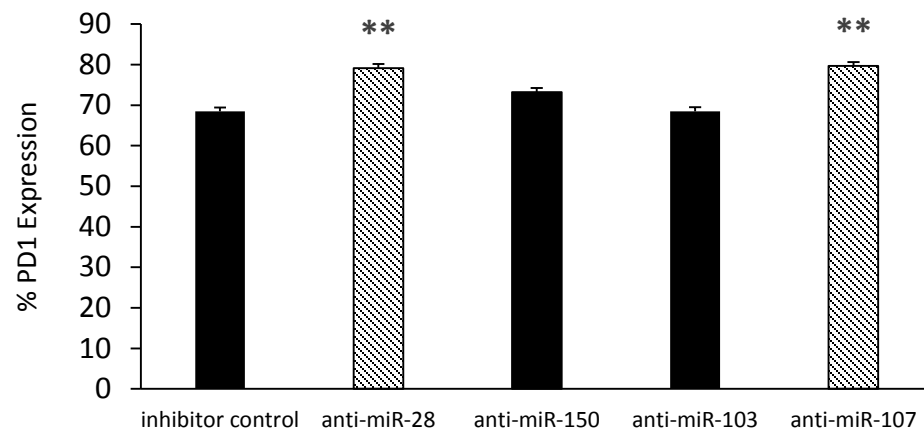
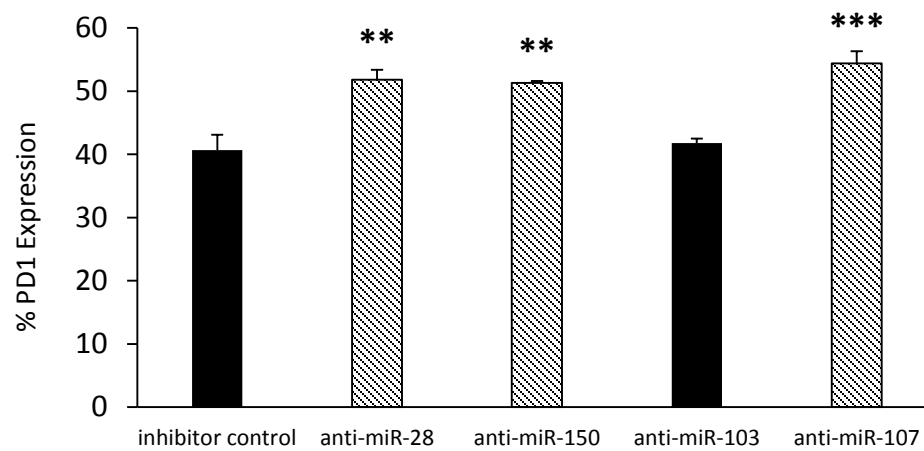
### 3.8 miR-28 and miR-107 mimic transfection has no effect on proliferation in CD4<sup>+</sup> T cells.

To investigate the therapeutic potential of miR-28 and miR-107, lymphocytes were transfected with 1  $\mu\text{g}$  of mimic control, miR-28 or miR-107 for 48 hours and stained with CFSE before a 4 day incubation on anti-CD3e coated plates (10  $\mu\text{g}/\text{mL}$ ). CD4<sup>+</sup> T cells were isolated using MACS beads and PD1 expression was analyzed to determine if these miRNA mimics can silence PD1 in T cells *in vitro*. While miR-107 had no significant effect on PD1 expression, miR-28 mimic reduced PD1 expression from 80.3% to 70.9% (Figure 3.14). To investigate whether this silencing resulted in altered proliferation the CD4<sup>+</sup> T cells were analyzed using flow cytometry with CFSE staining. By gating on CFSE<sup>low</sup> cells, the proportion of proliferating cells was analyzed between miRNA mimics and control (Figure 3.15A). No significant difference in the percent of proliferating cells was found between the control or miR-28/miR-107 mimic transfection (Figure 3.15B).

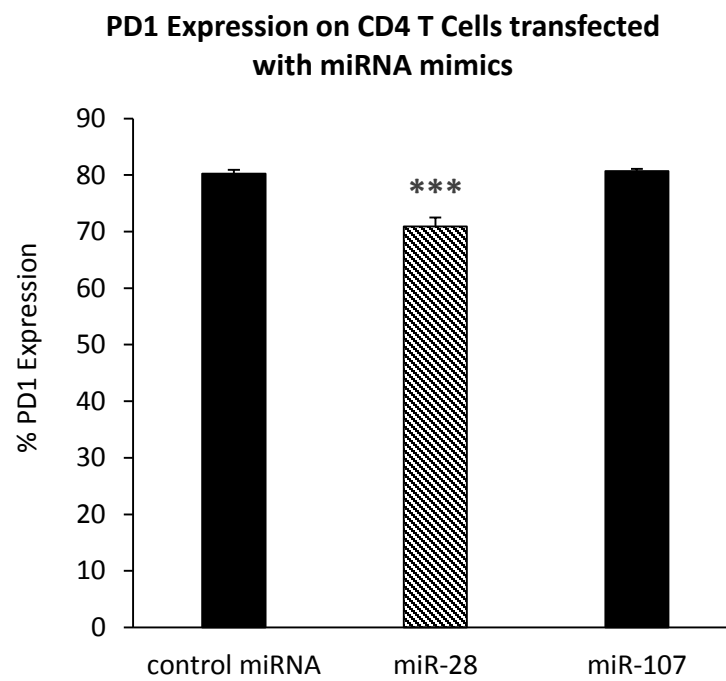
**Figure 3.12 A 2:1 ratio of GAPDH siRNA ( $\mu\text{g}$ ):Lipofectamine 2000 ( $\mu\text{L}$ ) results in a 75% knockdown in GAPDH expression 48 hours after transfection.** Using 1  $\mu\text{g}$  of GAPDH siRNA or control siRNA with a 2:1 ratio of siRNA:Lipofectamine 2000 ( $\mu\text{g}$ : $\mu\text{L}$ ), 2 million lymphocytes isolated from the lymph nodes of WT C57BL/6 were transfected in a 24 well plate. 48 hours after transfection, T cells were purified and RNA was isolated for use in real time qPCR with oligomers for GAPDH and  $\beta$ -actin (reference gene). A one-way ANOVA and Dunnett's multiple comparison test was used to compare the control and GAPDH siRNA to the non-transfected cells (\* =  $p < 0.05$ ). Data are representative of four independent experiments.



**Figure 3.13 miR-28, miR-150 and miR-107 inhibitors increase PD1 expression after T cell transfection and incubation on anti-CD3e coated plates.** 2 million lymphocytes, collected from lymph nodes of WT C57BL/6 mice, were plated per well in a 24 well plate and transfected with 1  $\mu$ g of miRNA inhibitor or inhibitor control. Cells were transfected at 37 °C for 48 hours before being transferred to a 24 well plate coated with 10  $\mu$ g/mL of anti-CD3e for 4 days. Flow cytometric analysis was performed to determine the miRNAs ability to alter expression of PD1 on (A) CD4<sup>+</sup> and (B) CD8<sup>+</sup> T cells. A one-way ANOVA test was used to determine significance ( $p < 0.05$ ), significance between the miRNA inhibitors and inhibitor control was determined with a Dunnett's multiple comparison test. Bars marked with a \*\* denote  $p < 0.01$  and \*\*\* denote  $p < 0.001$ . The data shown are representative of three independent experiments.

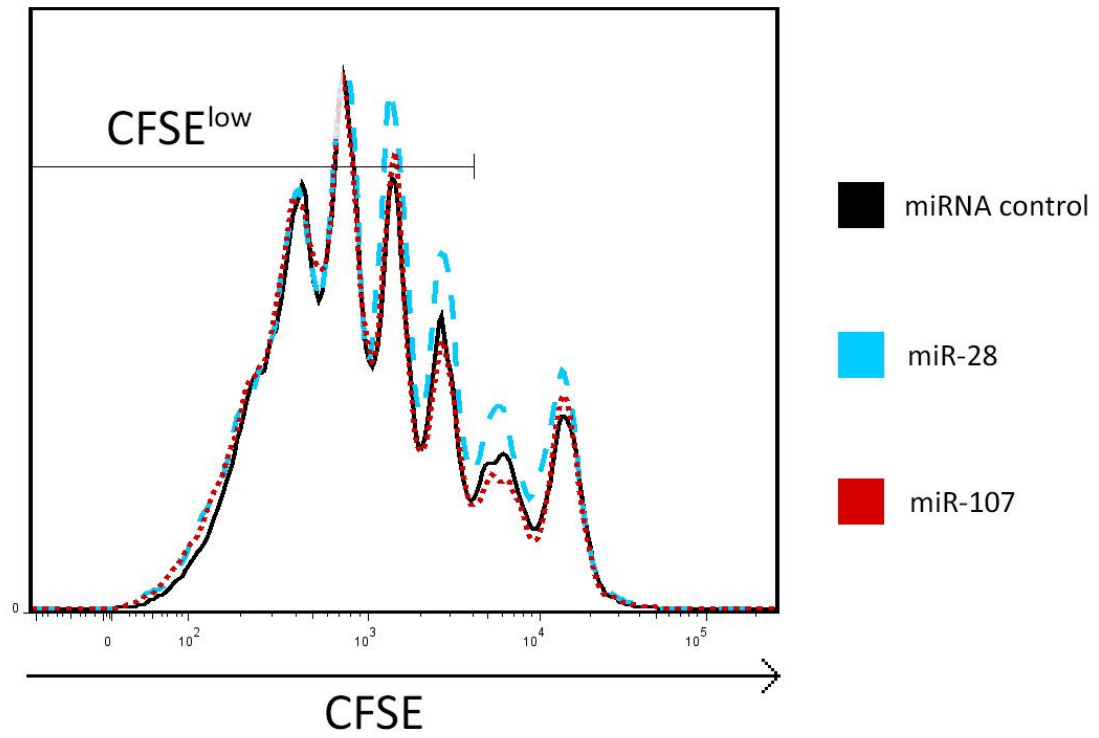
**A****PD1 Expression on CD4 T Cells transfected with miRNA inhibitors****B****PD1 Expression on CD8 T Cells transfected with miRNA inhibitors**

**Figure 3.14 miR-28 significantly silences PD1 expression in CD4<sup>+</sup> T cells after transfection and incubation on anti-CD3e coated plates.** Lymphocytes were isolated from lymph nodes of WT C57BL/6 mice and 2 million cells were plated per well in a 24 well plate. 1 µg of miRNA mimic or mimic control were transfected and cells were transfected at 37 °C for 48 hours before being transferred to a 24 well plate coated with 10 µg/mL of anti-CD3e for 4 days. CD4<sup>+</sup> T cells were isolated using MACS beads and flow cytometric analysis was performed to determine the miRNAs ability to silence expression of PD1 in T cells. Significance was determined using a one-way ANOVA followed by a Dunnett's multiple comparison test between control and each miRNA mimic (\*\*\*) =  $p < 0.001$ ). Data are representative of two independent experiments.

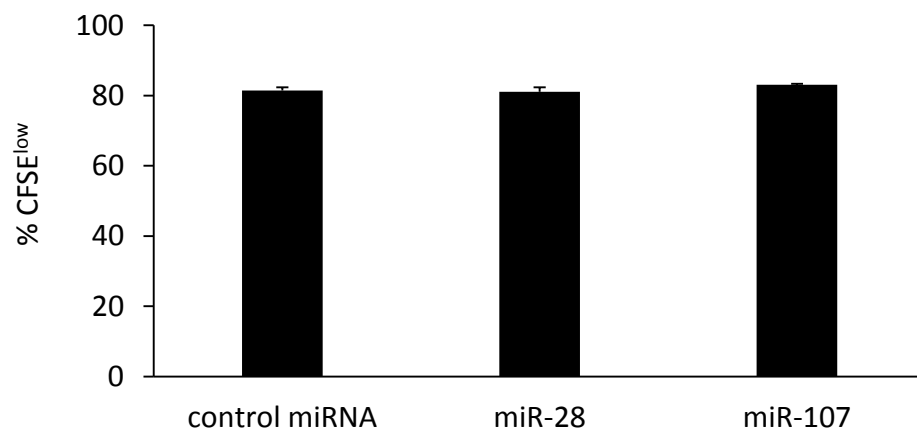


**Figure 3.15 miR-28 and miR-107 have no effect on cell proliferation induced by anti-CD3e stimulation.** 2 million lymphocytes, isolated from lymph nodes of WT C57BL/6 mice, were plated per well in a 24 well plate. 1  $\mu$ g of miRNA mimic or mimic control were transfected and cells were transfected at 37 °C for 48 hours. Cells were then stained with CFSE then plated on anti-CD3e coated plates (10  $\mu$ g/mL) for 4 days before CD4<sup>+</sup> T cell isolation, PD1-PerCP eFluor710 staining and flow cytometric analysis. (A) 4 day CFSE histogram showing the proliferation profiles of mimic control, miR-28 and miR-107 transfected T cells. (B) Quantification of the percentage of proliferated T cells (CFSE<sup>low</sup>). Significance ( $p < 0.05$ ) was determined using a one-way ANOVA followed by a Tukey's post-hoc test. Data shown are representative of four independent experiments.



**A****B**

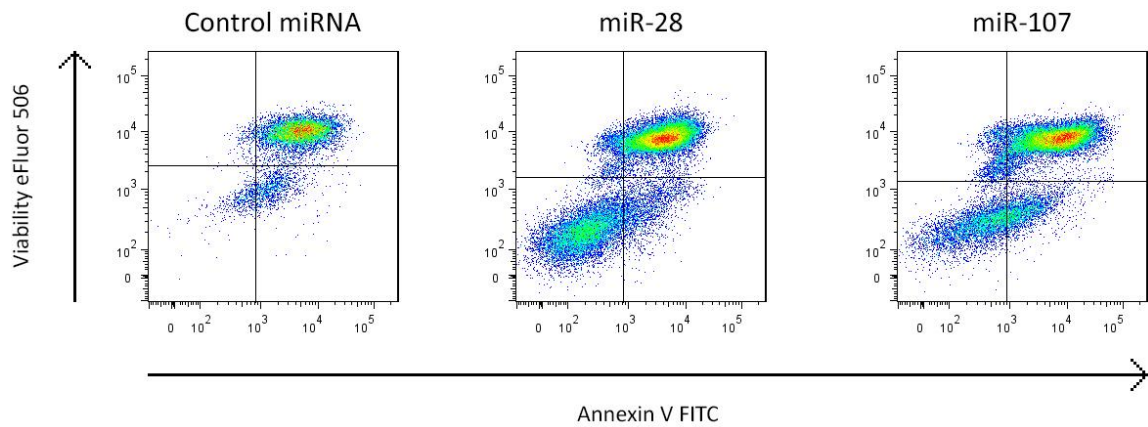
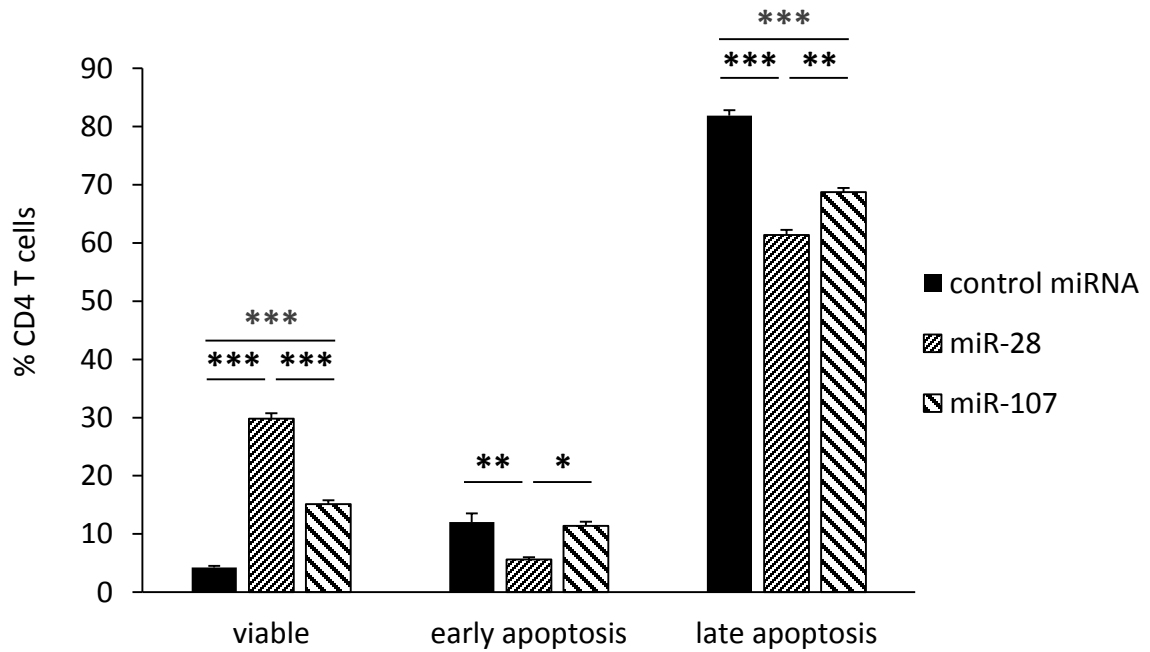
**Proliferation of CD4 T cells transfected with miRNA mimics**



### 3.9 miR-28 mimic transfection reduces anti-CD3e induced early and late apoptosis in CD4<sup>+</sup> T cells

The last experiment was designed to determine if transfection of CD4<sup>+</sup> T cells with miRNA mimic could reduce apoptosis in activated T cells. Lymphocytes were transfected as described in 3.8, however, no cells were stained with CFSE before 4 day incubation on anti-CD3e coated plates. After incubation, CD4<sup>+</sup> T cells were isolated and stained for PD1, Viability Dye eFluor 506 and Annexin V-FITC. Cells that stain eFluor506<sup>-</sup> AnnexinV<sup>+</sup> are in early apoptosis, while cells that stain eFluor506<sup>+</sup> AnnexinV<sup>+</sup> are in late apoptosis. miR-107 transfection had a significantly increased percentage of viable CD4<sup>+</sup> T cells (15.13% > 4.22%) and decreased percentage of late apoptotic cells (68.73% < 81.87%) over control (Figure 3.16A and B). miR-28 transfected CD4<sup>+</sup> T cells displayed even greater reductions in apoptosis compared to control: viability increased from 4.22% to 29.83%, early apoptosis decreased from 12.07% to 5.62% and late apoptosis decreased from 81.87% to 61.37% (Figure 3.16A and B).

**Figure 3.16 miR-28 mimic transfection significantly reduces the percentage of cells in early and late apoptosis caused by prolonged anti-CD3e activation.** Lymphocytes were isolated from lymph nodes of WT C57BL/6 mice and 2 million T cells were plated per well in a 24 well plate. 1  $\mu$ g of miRNA mimic or mimic control were transfected and cells were cultured at 37 °C for 48 hours before being plated on anti-CD3e coated plates (10  $\mu$ g/mL) for 4 days. Using CD4 MACS beads, CD4<sup>+</sup> T cells were purified and stained with PD1-PerCP eFluor710, viability dye eFluor 506 and annexin V FITC and analyzed by flow cytometry. **(A)** Dot plot showing viable (eFluor506<sup>-</sup>annexinV<sup>-</sup>), early apoptotic (eFluor506<sup>-</sup>annexinV<sup>+</sup>) and late apoptotic (eFluor506<sup>+</sup>annexinV<sup>+</sup>) CD4<sup>+</sup> T cells after transfection with mimic control, miR-28 or miR-107 and 4 day treatment with anti-CD3e. **(B)** Quantification of the viable, early and late apoptotic CD4<sup>+</sup> T cells. Within each stage of apoptosis, the miRNA mimics and controls were compared using a one-way ANOVA followed by Tukey's post-hoc test (\* =  $p < 0.05$ , \*\* =  $p < 0.01$  and \*\*\* =  $p < 0.001$ ). Data are representative of three independent experiments.

**A****B** Apoptosis of CD4 T cells transfected with miRNA mimics

## Chapter 4

### 4 Discussion

#### 4.1 Discussion

The key findings from this study are: 1) miR-28, miR-150 and miR-151-5p are downregulated; and miR-let-7e, miR-103, miR-107, miR-27a, miR-23a, miR-21, miR-155 and miR-146a are upregulated in PD1<sup>+</sup>CD4<sup>+</sup> T cells, 2) *in silico* data reveal that miR-28 and miR-150 should bind to the 3' UTRs of PD1, TIM3 and BTLA, while miR-103 and miR-107 bind to PD1 and BTLA, 3) anti-CD3e treatment upregulates PD1 expression and decreases expression of all 4 candidate miRNAs, 4) miR-28 and miR-107 bind to the 3' UTR of PD1 and silence PD1 expression, while lymphocyte transfection with miR-28, miR-150 and miR-107 inhibitors increase PD1 expression on T cells and 5) although no differences in proliferation were seen in miRNA mimic transfected CD4<sup>+</sup> T cells, miR-28 and miR-107 transfection lead to reduced early and late activation-induced apoptosis.

miRNAs are quietly emerging as new therapeutic markers for use in various diseases. Currently, two miRNA based therapeutics are in clinical trials that use a LNA anti-miR-122, miravirsen, against hepatitis C [106] or liposome-based miR-34a mimic, MRX34, against a multitude of cancers [107]. Although it is exciting to see the emergence of a new class of drugs for use in cancer therapy, miRNAs have their limitations. Although a miRNA may be able to target multiple genes in pro-tumoral pathways to elicit a broad anti-tumor responses, the possibility also exists for negative off-target effects [108]. As well, a miRNA may have separate targets in different cell types, i.e. cancer vs an immune cell, which can be beneficial or harmful as a therapeutic approach.

One of the most important factors that contribute to the success of RNAi therapies is the ability to deliver small RNA molecules inside the cell. A high transfection efficiency is necessary to ensure that the RNA has a significant effect on cell function, while a low toxicity is important to ensure that the therapeutic benefits of gene silencing outweigh the

cell loss due to transfection. T cells are difficult to transfect, and currently the most popular method to transfect primary human and murine T cells with siRNA/miRNA *in vitro* is electroporation. Electroporation uses an electric field to disrupt the cell membrane and allow RNA to enter the cell [109]. The industrial leader in T cell electroporation is Lonza with the Lonza Nucleofector II electroporation system and Amaxa Nucleofector Kits. When comparing homemade buffers to the ones found in the Amaxa Nucleofector Kit for human and murine T cells, Chicaybam *et al.* discovered that the Amaxa kit was superior at transfecting human T cells with approximately 45% transfection efficiency and 70% viability. On the other hand, the homemade buffer was superior at transfecting murine T cells with the transfection efficiency and viability at 40% and 60%, respectively [110]. In this study, a 2:1 ratio of siRNA ( $\mu\text{g}$ ):Lipofectamine 2000 ( $\mu\text{L}$ ) resulted in a greater murine T cell transfection efficiency of 62.7% and reduced total viability of 29.8% when compared to the Amaxa or homemade electroporation kits (Figure 3.11). Overall, the lipofectamine protocol may prove more versatile since electroporation is limited to transfecting activated T cells only; non-activated T cells demonstrated below 10% transfection efficiency and viability [110]. Other mentionable factors that lead to increased viability were the addition of 2-ME, a reducing agent that prevents oxygen radical buildup, and absence of penicillin or streptomycin in the transfection medium as per manufacturer's instructions.

Another issue that arose in this study was naturally low expression of PD1 on T cells from WT C57BL/6 mice. In order to demonstrate silencing of PD1, and how that affects the function of CD4<sup>+</sup> T cells, PD1 expression needed to be induced. One study conducted by Park *et al.* generated  $\gamma$ -retroviral vectors for expression of artificial miRNAs and transfected the vector into human lymphocytes along with one for constitutive expression of PD1 [111]. Of importance, miR-150 was able to silence vector-induced PD1 expression by approximately 90% 5 days after lymphocyte culture. It must be kept in mind, however, that the artificial vectors were created by designing a hybrid RNA molecule that resembles the endogenous miRNA with the stem sequence replaced by a siRNA against PD1. Consequently, the large silencing effect seen may be over-exaggerated by the presence of PD1 siRNA. As well, since human T cells were used for transduction and the analysis was conducted using flow cytometry, it is unknown whether

the miR-150 directly bound the PD1 transcript or indirectly silenced PD1. Therefore, this research project is the first to demonstrate that not only do miR-28 and miR-107 directly regulate PD1 expression through its 3' UTR, but miR-150 also indirectly silences PD1 in T cells through some unknown pathway. In order to avoid T cell transfection with miRNAs and a large vector, it was decided to use other means to induce PD1 expression. Anti-CD3e was chosen based on previous research that successfully used anti-CD3e to induced PD1 expression and T cell anergy on CD4<sup>+</sup> T cells to test the therapeutic effects of PD1 siRNA [29]. IFN $\gamma$  was tested based on curiosity since it can induce PD-L1 expression on B16 melanoma cells and other cancers [112-114].

In the past decade miRNA research has exploded and been explored as diagnostic, prognostic and therapeutic makers, but to date very little miRNA research exists on PD1, and none exist in the scope of melanoma therapy. One of the first miRNA and PD1 papers, written by Iliopoulos *et al.*, discovered that miR-21 was significantly upregulated upon ovalbumin stimulation in T cells, and that inhibition of PD1 with siRNA or knockout mice increased miR-21 expression [115]. As well, that miR-21 was found to control PDCD4, an intracellular protein with similar inhibitory effects as PD1 [115]. Recent studies on miR-21 and T cell activation demonstrate increased miR-21 expression in active or differentiated T cells [116, 117]. In this study, miR-21 was increased 10-fold in PD1<sup>+</sup>CD4<sup>+</sup> T cells, which is comparable to the miR-21 expression before and after ovalbumin stimulation. This paints the picture that tumor-specific T cells in the tumor microenvironment would activate, upregulate miR-21 and PD1, which results in PD1 silencing miR-21 and inducing the tumor suppressor targets of miR-21: PDCD4, PTEN and Bcl-2 [118]. In terms of T cell exhaustion, high miR-21 expression is considered therapeutic as it prevents upregulation of suppressor genes in the T cells; however, for many different cancers cells miR-21 is considered an oncomir as it supports continued cell growth. Therefore, if miRNA hope to have a place in immunotherapy then cell specific delivery techniques need to be in place to ensure removal of immune suppression in T cells while preventing miR-21-induced tumor-suppressor silencing in cancer cells. Moreover, it seems that miR-21 has altered regulating roles depending on the differentiation status of the CD4<sup>+</sup> T cell. Memory T cells have miR-21 function anti-apoptotically, while miR-21 in newly activated T cells silence CCR7 and modulates

lymphoid organ migration [119]. Therefore, specific delivery of miRNA into T cells may also be limited by specific subset delivery.

Other miRNAs of relevance in cancer immunotherapy are miR-150, miR-155 and miR146a. In this study, miR-150 expression was significantly decreased in PD1<sup>+</sup> T cells and shown to indirectly regulate PD1 expression. miR-150 mimic displayed no direct silencing of the 3' UTR of PD1 in the dual luciferase assay, but miR-150 inhibitors increased PD1 expression in T cells. Other studies reveal that miR-150 is downregulated in T cell lymphoma and colorectal cancer and is a tumor suppressor by targeting c-Myb [57, 120]. Conversely, in bladder cancer miR-150 is upregulated which results in lower PDCD4 expression [121]. Thus, miR-150 can be seen as a double edge sword as it acts as a tumor suppressor by silencing the oncogene c-Myb, while at the same time acting as an oncomir by silencing PDCD4 and increasing cell invasiveness. Overall, this strengthens the idea that miRNA regulation can be specific for different cell types and disease states, and therefore results from other studies on miRNAs and cancer may not necessarily translate to the field of melanoma immunotherapy.

miR-155 and miR-146a were the most altered in PD1<sup>+</sup> cells with approximately 12 and 21 fold increase, respectively. miR-155 is an interesting miRNA as it has been shown to silence CTLA4 [122], and miR-155 knockout mice are highly resistant to autoimmunity, which is reversed in miR-155(-/-)Pdc1(-/-) double knockout mice [123]. Upon T cell activation miR-155 has been shown to increase in expression and silence suppressor of cytokine signaling 1 (SOCS1) [124]. Thus, miR-155 is normally induced upon activated T cells and has two silencing pathways to support cell proliferation and maturation. miR-146a is normally low in naïve human T cells and is induced upon T cell receptor stimulation [125, 126]. Moreover, miR-146a expression is correlated to decreases in activation-induced cell death by targeting fas-associated death domain (FADD) [125]. However, similar to miR-150, miR-146a acts as a double edge sword to T cell growth and survival by targeting and silencing IL-2 through IRAK1 and TRAF6 [125] and inhibiting NF-κB activity, thus preventing hyperactivity in antigenic responses [126].



miR-23a recently has become a popular regulator of cytotoxicity in CD8<sup>+</sup> T cells. TGF- $\beta$  derived from tumors tissue upregulates miR-23a in CD8<sup>+</sup> T cells resulting in silencing of BLIMP-1, a promoter of cytotoxicity. From this discovery an effective adoptive cell therapy was created in mice by transfecting tumor-specific CD8<sup>+</sup> T cells with miR-23a inhibitor, resulting in reduced tumor growth [127]. Another study on miR-23a in CD8<sup>+</sup> T cells also found that increased miR-23a expression induced attenuation of cytotoxicity, which may be due to silencing of lysosomal-associated membrane protein 1 (LAMP1) [128]. In the same study, miR-27a was shown to directly silence IFN $\gamma$  acting as a partner to miR-23a to lower cytotoxicity upon TGF- $\beta$  stimulation. Although increases in miR-23a and miR-27a expression were observed in CD4<sup>+</sup>PD1<sup>+</sup> T cells, it is difficult to tell if miR-23a and miR-27a exhibit suppressive functions in CD4<sup>+</sup> T cells. Studies so far have only looked at miR-23a and miR-27a in CD8<sup>+</sup> T cells by investigating changes in cytotoxicity, and therefore no data is available to confirm if these miRNAs affect CD4<sup>+</sup> T cell function.

The previously mentioned miRNAs have been studied extensively in T cells and in cancer, and they demonstrate the delicate nature of a miRNA therapy in T cells. Due to the dual and opposite functions that miRNA can elicit, some miRNAs may have undesired off-target effects that can reduce the therapeutic benefits of miRNA regulation. Moreover, miRNAs can alter function depending on the cell-type transfected, thus efficient targeted delivery may be mandatory in order to observe functional changes or reduce off-target effects. Moving forward, the aim of this research was to discover miRNA that silence PD1 expression, which is why miR-28, miR-150, miR-103 and miR-107 were chosen for further study.

To date, almost no papers exist that focus on the function of miR-103 and miR-107 in T cells. One study, although focused on triple-negative breast cancer, analyzed the prognostic performance of miRNAs in 58 patients and found that lymph node status was the only clinicopathological factors that was significant in predicting poor prognosis. As well, that poor prognosis and distant metastasis were correlated to high intratumoral miR-103 and miR-107 expression [129]. Other research groups compared serum miRNA levels between breast cancer and healthy patients, and found elevated miR-107 levels

[130, 131]. Similar results were seen in lung and pancreatic cancer, where miR-107 was associated with tumor growth and decreased lung cancer survival and miR-103 was associated with risk of pancreatic cancer, however, miR-107 and miR-103 were lower in cancerous tissue [132, 133]. The prognostic potential of these miRNAs is not limited to disease progression, but extends towards therapeutic outcome prediction. Another study aimed to detect if miRNA levels can be used to predict outcomes of chemotherapy. Patients with metastatic colorectal cancer were treated with chemotherapy and intratumoral miRNA levels were measured. It was discovered that high miR-107 correlated to overall survival [134]. Plenty of evidence exists to confirm the prognostic potential of miR-103 and miR-107, however it appears expression changes seem to differ depending on the disease. This may be due to the fact that, similar to miR-150 and miR-146a, both miR-103 and miR-107 can act as oncomirs or tumor suppressive miRNAs by targeting DICER, PTEN or CCND1, CDK8, MCL1, PD1 respectively [134-137]. In this study, miR-103 and miR-107 was approximately 3-fold increased in PD1<sup>+</sup>CD4<sup>+</sup> T cells over PD1<sup>-</sup>CD4<sup>+</sup> T cells isolated from tumor-bearing mice, however, when CD4<sup>+</sup> T cells are stimulated with anti-CD3e for 24 hours expression of miR-103 and miR-107 decreased. Therefore, the increased miR-103 and miR-107 expression observed in PD1<sup>+</sup> cells may either be a result of the presence of melanoma or a marker of exhausted T cells.

miR-28 became the candidate miRNA that fulfilled the objectives of this study. Reductions were seen in PD1<sup>+</sup>CD4<sup>+</sup> T cells, miR-28 was shown to silence the 3' UTR of PD1 and use of miR-28 mimic and inhibitors altered PD1 expression resulting in the most significant decrease in activation-induced cell death. Current research involving miR-28 and T cell disease primarily focuses on HIV infection, but one research article on natural killer/T-cell lymphoma (NKTL) demonstrated reductions in miR-28 expression in cancerous cells. However, transfection with miR-28 mimic reduced cell growth in NKTL cells [138]. When looking at a different immune cell, the B cell, miR-28 expression is reduced in B cell lymphoma and reexpression of this miRNA leads to impaired cell proliferation through MAD2L1, a component of the cell cycle through mitotic spindle coordination [139]. With focus on a non-immune cell related cancer, clear cell renal cell carcinoma, miR-28 mimic transfection was shown to weaken mitotic checkpoint activation and induce chromosomal instability by also targeting MAD2L1 [140].

Although miR-28 reexpression in my study proved beneficial to CD4<sup>+</sup> T cells, these contradicting results illustrate the necessity to further understand altered miRNA expression between subsets of T cells (CD4<sup>+</sup> vs CD8<sup>+</sup> or NK cells), as well as between whether the T cell is the origin of the disease or merely a combatant in the fight against cancer. In the end, the fact cannot be ignored that miR-28 is downregulated in a multitude of cancerous immune cells and tissues, and maintains a tumor suppressive role by reducing growth of cancerous cells through MAD2L1. This research project expands the role of miR-28 as an indirect tumor suppressor by preventing cell death in activated CD4<sup>+</sup> T cells through silenced PD1 expression.

In conclusion, miR-28 and miR-107 were shown to silence PD1 through its 3' UTR, and transfection with miR-28 and miR-107 mimics reduced early and late activation-induced cell death. Therefore, miR-28 and miR-107 remain as great candidates to act as a silencing therapeutic agent against PD1. Ultimately, this novel research demonstrates a potential role for miR-28 and miR-107 in regulating T cell responses to cancer. With the success that anti-PD1 antibodies are having in clinical trials, investigating how miRNA regulates PD1 in T cells is necessary to expand our understanding of immunoregulatory pathways for prognostic and therapeutic purposes.

## 4.2 Future Directions

In this thesis, the microarray profile between PD1<sup>+/-</sup> CD4<sup>+</sup> T cell allowed us to discover, for the first time, miRNAs from a murine melanoma model that alter expression based on PD1 status. With a focus towards reversing T cell suppression caused by melanoma, various miRNAs were highlighted as candidates to silence PD1 and other T cell exhaustion markers. However, more can be done to further understand how miR-28 and miR-107 regulate T cell function *in vitro*. For instance, an ELISA or intracellular flow cytometry staining of IFN $\gamma$ , TNF $\alpha$  and IL-2 after miRNA mimic/inhibitor transfection is recommended to determine if these miRNA can increase anti-tumoral cytokine secretion. Moreover, to understand how miR-28 and miR-107 affect CD8-mediated cytotoxicity, a

cytotoxic T lymphocyte killing assay can be performed using miRNA-transfected CD8<sup>+</sup> T cells and labelled B16F10 cells.

In order to determine if any of the candidate miRNA affect TIM3 or BTLA expression, the pmirGLO dual luciferase assay should be utilized in tandem with miRNA mimic/inhibitor transfection of T cells. The dual luciferase assay displays miRNAs that directly bind to the 3' UTR, while *in vitro* T cell transfection provides a more physiological relevant microenvironment to confirm direct and indirect expression changes.

The final step for this study would involve a translation to *in vivo* murine melanoma model to discover if these miRNAs can improve T cell function against B16F10 melanoma. Evidence has shown that miRNAs may have opposing functions in different cell types, therefore a T cell specific delivery system is necessary to minimize the off-target effects of the miRNA candidates. Many new methods are coming to fruition by using CD7 antibody conjugated to oligo-9-arginine (scFvCD7-9R), CD7 antibody conjugated to chitosan or RNA-secreting primary B lymphocytes to deliver RNA into T cells [124, 141-143]. Alternatively, to avoid the barrier of specific T cell gene delivery *in vivo*, current *in vitro* methods can be used to transfect T cells for adoptive cell transfer. If altering expression of miRNAs, such as miR-28 and miR-107, in T cells can demonstrate control of T cell function towards melanoma in a mouse model, it would warrant translation to human T lymphocytes from melanoma patients.

## Chapter 5

### 5 References

1. Statistics, C.C.S.s.A.C.o.C. (2014). Canadian Cancer Statistics 2014. *Canadian Cancer Society*. Toronto, ON.
2. Satyamoorthy, K. and M. Herlyn. (2002). Cellular and molecular biology of human melanoma. *Cancer Biol Ther.* **1**, 14-7.
3. Hoerter, J.D., et al. (2012). Extrafollicular dermal melanocyte stem cells and melanoma. *Stem Cells Int.* **2012**, 407079.
4. Jimbow, K., et al. (1976). Some aspects of melanin biology: 1950-1975. *J Invest Dermatol.* **67**, 72-89.
5. Linsley, P.S., et al. (1992). Immunosuppression in vivo by a soluble form of the CTLA-4 T cell activation molecule. *Science.* **257**, 792-5.
6. Jang, A. and R.P. Hill. (1991). Drug sensitivity and metastatic ability in B16 melanoma cells. *Clin Exp Metastasis.* **9**, 393-402.
7. Eggermont, A.M. and C. Robert. (2011). New drugs in melanoma: it's a whole new world. *Eur J Cancer.* **47**, 2150-7.
8. Middleton, M.R., et al. (2000). Randomized phase III study of temozolomide versus dacarbazine in the treatment of patients with advanced metastatic malignant melanoma. *J Clin Oncol.* **18**, 158-66.
9. Wheatley, K., et al. (2003). Does adjuvant interferon-alpha for high-risk melanoma provide a worthwhile benefit? A meta-analysis of the randomised trials. *Cancer Treat Rev.* **29**, 241-52.
10. Atkins, M.B., et al. (2000). High-dose recombinant interleukin-2 therapy in patients with metastatic melanoma: long-term survival update. *Cancer J Sci Am.* **6**, S11-4.
11. Atkins, M.B., et al. (2008). Phase III trial comparing concurrent biochemotherapy with cisplatin, vinblastine, dacarbazine, interleukin-2, and interferon alfa-2b with cisplatin, vinblastine, and dacarbazine alone in patients with metastatic malignant melanoma (E3695): a trial coordinated by the Eastern Cooperative Oncology Group. *J Clin Oncol.* **26**, 5748-54.
12. Long, G.V., et al. (2011). Prognostic and clinicopathologic associations of oncogenic BRAF in metastatic melanoma. *J Clin Oncol.* **29**, 1239-46.

13. Chan, M.M., et al. (2014). The nature and management of metastatic melanoma after progression on BRAF inhibitors: effects of extended BRAF inhibition. *Cancer*. **120**, 3142-53.
14. Sosman, J.A., et al. (2012). Survival in BRAF V600-mutant advanced melanoma treated with vemurafenib. *N Engl J Med*. **366**, 707-14.
15. Davies, H., et al. (2002). Mutations of the BRAF gene in human cancer. *Nature*. **417**, 949-54.
16. Bowyer, S.E., et al. (2014). Activity of trametinib in K601E and L597Q BRAF mutation-positive metastatic melanoma. *Melanoma Res*. **24**, 504-8.
17. Menzies, A.M. and G.V. Long. (2014). Dabrafenib and trametinib, alone and in combination for BRAF-mutant metastatic melanoma. *Clin Cancer Res*. **20**, 2035-43.
18. Kim, K.B., et al. (2012). BEAM: a randomized phase II study evaluating the activity of bevacizumab in combination with carboplatin plus paclitaxel in patients with previously untreated advanced melanoma. *J Clin Oncol*. **30**, 34-41.
19. Kluger, H.M., et al. (2011). A phase 2 trial of dasatinib in advanced melanoma. *Cancer*. **117**, 2202-8.
20. Eggermont, A., et al. (2014). Harnessing the immune system to provide long-term survival in patients with melanoma and other solid tumors. *Oncoimmunology*. **3**, e27560.
21. Mamalis, A., M. Garcha, and J. Jagdeo. (2014). Targeting the PD-1 pathway: a promising future for the treatment of melanoma. *Arch Dermatol Res*. **306**, 511-9.
22. Baitsch, L., et al. (2012). Extended co-expression of inhibitory receptors by human CD8 T-cells depending on differentiation, antigen-specificity and anatomical localization. *PLoS One*. **7**, e30852.
23. Barber, D.L., et al. (2006). Restoring function in exhausted CD8 T cells during chronic viral infection. *Nature*. **439**, 682-7.
24. Blackburn, S.D., et al. (2008). Selective expansion of a subset of exhausted CD8 T cells by alphaPD-L1 blockade. *Proc Natl Acad Sci U S A*. **105**, 15016-21.

25. Ahmadzadeh, M., et al. (2009). Tumor antigen-specific CD8 T cells infiltrating the tumor express high levels of PD-1 and are functionally impaired. *Blood*. **114**, 1537-44.
26. Blank, C., et al. (2006). Blockade of PD-L1 (B7-H1) augments human tumor-specific T cell responses in vitro. *Int J Cancer*. **119**, 317-27.
27. Gehring, A.J., et al. (2009). Profile of tumor antigen-specific CD8 T cells in patients with hepatitis B virus-related hepatocellular carcinoma. *Gastroenterology*. **137**, 682-90.
28. Iwamura, K., et al. (2012). siRNA-mediated silencing of PD-1 ligands enhances tumor-specific human T-cell effector functions. *Gene Ther*. **19**, 959-66.
29. Bishop, K.D., et al. (2009). Depletion of the programmed death-1 receptor completely reverses established clonal anergy in CD4(+) T lymphocytes via an interleukin-2-dependent mechanism. *Cell Immunol*. **256**, 86-91.
30. Borkner, L., et al. (2010). RNA interference targeting programmed death receptor-1 improves immune functions of tumor-specific T cells. *Cancer Immunol Immunother*. **59**, 1173-83.
31. Sakuishi, K., et al. (2010). Targeting Tim-3 and PD-1 pathways to reverse T cell exhaustion and restore anti-tumor immunity. *J Exp Med*. **207**, 2187-94.
32. Fourcade, J., et al. (2010). Upregulation of Tim-3 and PD-1 expression is associated with tumor antigen-specific CD8+ T cell dysfunction in melanoma patients. *J Exp Med*. **207**, 2175-86.
33. Zhou, Q., et al. (2011). Coexpression of Tim-3 and PD-1 identifies a CD8+ T-cell exhaustion phenotype in mice with disseminated acute myelogenous leukemia. *Blood*. **117**, 4501-10.
34. Ngiow, S.F., et al. (2011). Anti-TIM3 antibody promotes T cell IFN-gamma-mediated antitumor immunity and suppresses established tumors. *Cancer Res*. **71**, 3540-51.
35. Fourcade, J., et al. (2012). CD8(+) T cells specific for tumor antigens can be rendered dysfunctional by the tumor microenvironment through upregulation of the inhibitory receptors BTLA and PD-1. *Cancer Res*. **72**, 887-96.

36. Ishida, Y., et al. (1992). Induced expression of PD-1, a novel member of the immunoglobulin gene superfamily, upon programmed cell death. *Embo j.* **11**, 3887-95.
37. Yamazaki, T., et al. (2002). Expression of programmed death 1 ligands by murine T cells and APC. *J Immunol.* **169**, 5538-45.
38. Chemnitz, J.M., et al. (2004). SHP-1 and SHP-2 associate with immunoreceptor tyrosine-based switch motif of programmed death 1 upon primary human T cell stimulation, but only receptor ligation prevents T cell activation. *J Immunol.* **173**, 945-54.
39. Okazaki, T., et al. (2001). PD-1 immunoreceptor inhibits B cell receptor-mediated signaling by recruiting src homology 2-domain-containing tyrosine phosphatase 2 to phosphotyrosine. *Proc Natl Acad Sci U S A.* **98**, 13866-71.
40. Parry, R.V., et al. (2005). CTLA-4 and PD-1 receptors inhibit T-cell activation by distinct mechanisms. *Mol Cell Biol.* **25**, 9543-53.
41. Pardoll, D.M. (2012). The blockade of immune checkpoints in cancer immunotherapy. *Nat Rev Cancer.* **12**, 252-64.
42. Dong, H., et al. (1999). B7-H1, a third member of the B7 family, co-stimulates T-cell proliferation and interleukin-10 secretion. *Nat Med.* **5**, 1365-9.
43. Freeman, G.J., et al. (2000). Engagement of the PD-1 immunoinhibitory receptor by a novel B7 family member leads to negative regulation of lymphocyte activation. *J Exp Med.* **192**, 1027-34.
44. Latchman, Y., et al. (2001). PD-L2 is a second ligand for PD-1 and inhibits T cell activation. *Nat Immunol.* **2**, 261-8.
45. Tseng, S.Y., et al. (2001). B7-DC, a new dendritic cell molecule with potent costimulatory properties for T cells. *J Exp Med.* **193**, 839-46.
46. Loke, P. and J.P. Allison. (2003). PD-L1 and PD-L2 are differentially regulated by Th1 and Th2 cells. *Proc Natl Acad Sci U S A.* **100**, 5336-41.
47. Kuchroo, V.K., et al. (2006). TIM family of genes in immunity and tolerance. *Adv Immunol.* **91**, 227-49.
48. Monney, L., et al. (2002). Th1-specific cell surface protein Tim-3 regulates macrophage activation and severity of an autoimmune disease. *Nature.* **415**, 536-41.



49. Sabatos, C.A., et al. (2003). Interaction of Tim-3 and Tim-3 ligand regulates T helper type 1 responses and induction of peripheral tolerance. *Nat Immunol.* **4**, 1102-10.
50. Sanchez-Fueyo, A., et al. (2003). Tim-3 inhibits T helper type 1-mediated auto- and alloimmune responses and promotes immunological tolerance. *Nat Immunol.* **4**, 1093-101.
51. Li, X., et al. (2012). T cell immunoglobulin-3 as a new therapeutic target for rheumatoid arthritis. *Expert Opin Ther Targets.* **16**, 1145-9.
52. Zhu, C., et al. (2005). The Tim-3 ligand galectin-9 negatively regulates T helper type 1 immunity. *Nat Immunol.* **6**, 1245-52.
53. Chiba, S., et al. (2012). Tumor-infiltrating DCs suppress nucleic acid-mediated innate immune responses through interactions between the receptor TIM-3 and the alarmin HMGB1. *Nat Immunol.* **13**, 832-42.
54. Ndhlovu, L.C., et al. (2012). Tim-3 marks human natural killer cell maturation and suppresses cell-mediated cytotoxicity. *Blood.* **119**, 3734-43.
55. Su, E.W., J.Y. Lin, and L.P. Kane. (2008). TIM-1 and TIM-3 proteins in immune regulation. *Cytokine.* **44**, 9-13.
56. Zhang, Y., et al. (2012). Tim-3 regulates pro- and anti-inflammatory cytokine expression in human CD14<sup>+</sup> monocytes. *J Leukoc Biol.* **91**, 189-96.
57. Watanabe, N., et al. (2003). BTLA is a lymphocyte inhibitory receptor with similarities to CTLA-4 and PD-1. *Nat Immunol.* **4**, 670-9.
58. Hurchla, M.A., et al. (2005). B and T lymphocyte attenuator exhibits structural and expression polymorphisms and is highly induced in anergic CD4<sup>+</sup> T cells. *J Immunol.* **174**, 3377-85.
59. Krieg, C., et al. (2007). B and T lymphocyte attenuator regulates CD8<sup>+</sup> T cell-intrinsic homeostasis and memory cell generation. *Nat Immunol.* **8**, 162-71.
60. Melero, I., et al. (2013). Clinical development of immunostimulatory monoclonal antibodies and opportunities for combination. *Clin Cancer Res.* **19**, 997-1008.
61. Kyi, C. and M.A. Postow. (2014). Checkpoint blocking antibodies in cancer immunotherapy. *FEBS Lett.* **588**, 368-76.

62. Menzies, A.M. and G.V. Long. (2013). New combinations and immunotherapies for melanoma: latest evidence and clinical utility. *Ther Adv Med Oncol.* **5**, 278-85.
63. Lu, J., et al. (2014). Clinical evaluation of compounds targeting PD-1/PD-L1 pathway for cancer immunotherapy. *J Oncol Pharm Pract.* Epub ahead of print.
64. Lee, J.J., G.F. Murphy, and C.G. Lian. (2014). Melanoma epigenetics: novel mechanisms, markers, and medicines. *Lab Invest.* **94**, 822-38.
65. Bhattacharya, A., et al. (2013). Regulation of cell cycle checkpoint kinase WEE1 by miR-195 in malignant melanoma. *Oncogene.* **32**, 3175-83.
66. Rodriguez-Paredes, M. and M. Esteller. (2011). Cancer epigenetics reaches mainstream oncology. *Nat Med.* **17**, 330-9.
67. Kato, Y., et al. (2014). Combination of HDAC inhibitor MS-275 and IL-2 increased anti-tumor effect in a melanoma model via activated cytotoxic T cells. *J Dermatol Sci.* **75**, 140-7.
68. Bartel, D.P. (2004). MicroRNAs: genomics, biogenesis, mechanism, and function. *Cell.* **116**, 281-97.
69. Lee, R.C., R.L. Feinbaum, and V. Ambros. (1993). The *C. elegans* heterochronic gene *lin-4* encodes small RNAs with antisense complementarity to *lin-14*. *Cell.* **75**, 843-54.
70. Wightman, B., I. Ha, and G. Ruvkun. (1993). Posttranscriptional regulation of the heterochronic gene *lin-14* by *lin-4* mediates temporal pattern formation in *C. elegans*. *Cell.* **75**, 855-62.
71. Fire, A., et al. (1998). Potent and specific genetic interference by double-stranded RNA in *Caenorhabditis elegans*. *Nature.* **391**, 806-11.
72. Hamilton, A.J. and D.C. Baulcombe. (1999). A species of small antisense RNA in posttranscriptional gene silencing in plants. *Science.* **286**, 950-2.
73. Tomari, Y. and P.D. Zamore. (2005). Perspective: machines for RNAi. *Genes Dev.* **19**, 517-29.
74. Carthew, R.W. and E.J. Sontheimer. (2009). Origins and Mechanisms of miRNAs and siRNAs. *Cell.* **136**, 642-55.
75. Perera, R.J. and A. Ray. (2007). MicroRNAs in the search for understanding human diseases. *BioDrugs.* **21**, 97-104.

76. Kim, V.N. (2005). MicroRNA biogenesis: coordinated cropping and dicing. *Nat Rev Mol Cell Biol.* **6**, 376-85.
77. Eulalio, A., E. Huntzinger, and E. Izaurralde. (2008). Getting to the root of miRNA-mediated gene silencing. *Cell.* **132**, 9-14.
78. Chen, J., et al. (2011). miR-193b Regulates Mcl-1 in Melanoma. *Am J Pathol.* **179**, 2162-8.
79. Felicetti, F., et al. (2008). The promyelocytic leukemia zinc finger-microRNA-221/-222 pathway controls melanoma progression through multiple oncogenic mechanisms. *Cancer Res.* **68**, 2745-54.
80. Friedman, E.B., et al. (2012). Serum microRNAs as biomarkers for recurrence in melanoma. *J Transl Med.* **10**, 155.
81. Igoucheva, O. and V. Alexeev. (2009). MicroRNA-dependent regulation of cKit in cutaneous melanoma. *Biochem Biophys Res Commun.* **379**, 790-4.
82. Muller, D.W. and A.K. Bosserhoff. (2008). Integrin beta 3 expression is regulated by let-7a miRNA in malignant melanoma. *Oncogene.* **27**, 6698-706.
83. Penna, E., et al. (2011). microRNA-214 contributes to melanoma tumour progression through suppression of TFAP2C. *Embo j.* **30**, 1990-2007.
84. Dar, A.A., et al. (2011). miRNA-205 suppresses melanoma cell proliferation and induces senescence via regulation of E2F1 protein. *J Biol Chem.* **286**, 16606-14.
85. Dar, A.A., et al. (2013). The role of miR-18b in MDM2-p53 pathway signaling and melanoma progression. *J Natl Cancer Inst.* **105**, 433-42.
86. Kappelmann, M., et al. (2013). MicroRNA miR-125b controls melanoma progression by direct regulation of c-Jun protein expression. *Oncogene.* **32**, 2984-91.
87. Lodygin, D., et al. (2008). Inactivation of miR-34a by aberrant CpG methylation in multiple types of cancer. *Cell Cycle.* **7**, 2591-600.
88. Reuland, S.N., et al. (2013). MicroRNA-26a is strongly downregulated in melanoma and induces cell death through repression of silencer of death domains (SODD). *J Invest Dermatol.* **133**, 1286-93.
89. Wang, H.F., et al. (2013). miR-573 regulates melanoma progression by targeting the melanoma cell adhesion molecule. *Oncol Rep.* **30**, 520-6.

90. Luo, C., et al. (2014). The role of microRNAs in melanoma. *Eur J Cell Biol.* **93**, 11-22.
91. Bartels, C.L. and G.J. Tsongalis. (2009). MicroRNAs: novel biomarkers for human cancer. *Clin Chem.* **55**, 623-31.
92. Costinean, S., et al. (2006). Pre-B cell proliferation and lymphoblastic leukemia/high-grade lymphoma in E(mu)-miR155 transgenic mice. *Proc Natl Acad Sci U S A.* **103**, 7024-9.
93. Levati, L., et al. (2009). Altered expression of selected microRNAs in melanoma: antiproliferative and proapoptotic activity of miRNA-155. *Int J Oncol.* **35**, 393-400.
94. Segura, M.F., et al. (2010). Melanoma MicroRNA signature predicts post-recurrence survival. *Clin Cancer Res.* **16**, 1577-86.
95. Caramuta, S., et al. (2010). MicroRNA expression profiles associated with mutational status and survival in malignant melanoma. *J Invest Dermatol.* **130**, 2062-70.
96. Hanna, J.A., et al. (2012). In situ measurement of miR-205 in malignant melanoma tissue supports its role as a tumor suppressor microRNA. *Lab Invest.* **92**, 1390-7.
97. Satzger, I., et al. (2010). MicroRNA-15b represents an independent prognostic parameter and is correlated with tumor cell proliferation and apoptosis in malignant melanoma. *Int J Cancer.* **126**, 2553-62.
98. Bader, A.G., D. Brown, and M. Winkler. (2010). The promise of microRNA replacement therapy. *Cancer Res.* **70**, 7027-30.
99. Chen, Y., et al. (2010). Nanoparticles modified with tumor-targeting scFv deliver siRNA and miRNA for cancer therapy. *Mol Ther.* **18**, 1650-6.
100. Huynh, C., et al. (2011). Efficient in vivo microRNA targeting of liver metastasis. *Oncogene.* **30**, 1481-8.
101. Poell, J.B., et al. (2012). A functional screen identifies specific microRNAs capable of inhibiting human melanoma cell viability. *PLoS One.* **7**, e43569.
102. Kheirelseid, E.A., et al. (2013). miRNA expressions in rectal cancer as predictors of response to neoadjuvant chemoradiation therapy. *Int J Colorectal Dis.* **28**, 247-60.

103. Hodi, F.S., et al. (2010). Improved survival with ipilimumab in patients with metastatic melanoma. *N Engl J Med.* **363**, 711-23.
104. Livak, K.J. and T.D. Schmittgen. (2001). Analysis of relative gene expression data using real-time quantitative PCR and the 2(-Delta Delta C(T)) Method. *Methods.* **25**, 402-8.
105. Yang, W., et al. (2008). PD-L1: PD-1 interaction contributes to the functional suppression of T-cell responses to human uveal melanoma cells in vitro. *Invest Ophthalmol Vis Sci.* **49**, 2518-25.
106. Janssen, H.L., et al. (2013). Treatment of HCV infection by targeting microRNA. *N Engl J Med.* **368**, 1685-94.
107. Misso, G., et al. (2014). Mir-34: a new weapon against cancer? *Mol Ther Nucleic Acids.* **3**, e194.
108. Ling, H., M. Fabbri, and G.A. Calin. (2013). MicroRNAs and other non-coding RNAs as targets for anticancer drug development. *Nat Rev Drug Discov.* **12**, 847-65.
109. Freeley, M. and A. Long. (2013). Advances in siRNA delivery to T-cells: potential clinical applications for inflammatory disease, cancer and infection. *Biochem J.* **455**, 133-47.
110. Chicaybam, L., et al. (2013). An efficient low cost method for gene transfer to T lymphocytes. *PLoS One.* **8**, e60298.
111. Park, T.S., et al. (2014). Gamma-retroviral vector design for the co-expression of artificial microRNAs and therapeutic proteins. *Nucleic Acid Ther.* **24**, 356-63.
112. Chen, J., et al. (2012). Interferon-gamma-induced PD-L1 surface expression on human oral squamous carcinoma via PKD2 signal pathway. *Immunobiology.* **217**, 385-93.
113. Kronig, H., et al. (2014). Interferon-induced programmed death-ligand 1 (PD-L1/B7-H1) expression increases on human acute myeloid leukemia blast cells during treatment. *Eur J Haematol.* **92**, 195-203.
114. Spranger, S., et al. (2013). Up-regulation of PD-L1, IDO, and T(regs) in the melanoma tumor microenvironment is driven by CD8(+) T cells. *Sci Transl Med.* **5**, 200ra116.

115. Iliopoulos, D., et al. (2011). The negative costimulatory molecule PD-1 modulates the balance between immunity and tolerance via miR-21. *Eur J Immunol.* **41**, 1754-63.
116. Salaun, B., et al. (2011). Differentiation associated regulation of microRNA expression in vivo in human CD8+ T cell subsets. *J Transl Med.* **9**, 44.
117. Sommers, C.L., et al. (2013). miRNA signature of mouse helper T cell hyper-proliferation. *PLoS One.* **8**, e66709.
118. Wickramasinghe, N.S., et al. (2009). Estradiol downregulates miR-21 expression and increases miR-21 target gene expression in MCF-7 breast cancer cells. *Nucleic Acids Res.* **37**, 2584-95.
119. Smigielska-Czepiel, K., et al. (2013). Dual role of miR-21 in CD4+ T-cells: activation-induced miR-21 supports survival of memory T-cells and regulates CCR7 expression in naive T-cells. *PLoS One.* **8**, e76217.
120. Feng, J., et al. (2014). miR-150 functions as a tumour suppressor in human colorectal cancer by targeting c-Myb. *J Cell Mol Med.* **18**, 2125-34.
121. Lei, Y., et al. (2014). miR-150 modulates cisplatin chemosensitivity and invasiveness of muscle-invasive bladder cancer cells via targeting PDCD4 in vitro. *Med Sci Monit.* **20**, 1850-7.
122. Sonkoly, E., et al. (2010). MiR-155 is overexpressed in patients with atopic dermatitis and modulates T-cell proliferative responses by targeting cytotoxic T lymphocyte-associated antigen 4. *J Allergy Clin Immunol.* **126**, 581-9.e1-20.
123. Zhang, J. and M.Y. Braun. (2014). PD-1 deletion restores susceptibility to experimental autoimmune encephalomyelitis in miR-155-deficient mice. *Int Immunol.* **26**, 407-15.
124. Dudda, J.C., et al. (2013). MicroRNA-155 is required for effector CD8+ T cell responses to virus infection and cancer. *Immunity.* **38**, 742-53.
125. Curtale, G., et al. (2010). An emerging player in the adaptive immune response: microRNA-146a is a modulator of IL-2 expression and activation-induced cell death in T lymphocytes. *Blood.* **115**, 265-73.
126. Yang, L., et al. (2012). miR-146a controls the resolution of T cell responses in mice. *J Exp Med.* **209**, 1655-70.

127. Lin, R., et al. (2014). Targeting miR-23a in CD8+ cytotoxic T lymphocytes prevents tumor-dependent immunosuppression. *J Clin Invest*. Epub ahead of print.
128. Chandran, P.A., et al. (2014). The TGF-beta-inducible miR-23a cluster attenuates IFN-gamma levels and antigen-specific cytotoxicity in human CD8+ T cells. *J Leukoc Biol*. **96**, 633-45.
129. Shen, S., et al. (2014). A prognostic model of triple-negative breast cancer based on miR-27b-3p and node status. *PLoS One*. **9**, e100664.
130. Chen, P.S., et al. (2011). miR-107 promotes tumor progression by targeting the let-7 microRNA in mice and humans. *J Clin Invest*. **121**, 3442-55.
131. Kodahl, A.R., et al. (2014). Novel circulating microRNA signature as a potential non-invasive multi-marker test in ER-positive early-stage breast cancer: a case control study. *Mol Oncol*. **8**, 874-83.
132. Tian, Y., et al. (2014). Interaction of Serum microRNAs and Serum Folate With the Susceptibility to Pancreatic Cancer. *Pancreas*. Epub ahead of print.
133. Zhong, K.Z., et al. (2014). Clinicopathological and prognostic significance of microRNA-107 in human non small cell lung cancer. *Int J Clin Exp Pathol*. **7**, 4545-51.
134. Molina-Pinelo, S., et al. (2014). MiR-107 and miR-99a-3p predict chemotherapy response in patients with advanced colorectal cancer. *BMC Cancer*. **14**, 656.
135. Geng, L., et al. (2014). MicroRNA-103 promotes colorectal cancer by targeting tumor suppressor DICER and PTEN. *Int J Mol Sci*. **15**, 8458-72.
136. Song, Y.Q., et al. (2014). MicroRNA-107 promotes proliferation of gastric cancer cells by targeting cyclin dependent kinase 8. *Diagn Pathol*. **9**, 164.
137. Zhou, C., et al. (2014). miR-107 Activates ATR/Chk1 Pathway and Suppress Cervical Cancer Invasion by Targeting MCL1. *PLoS One*. **9**, e111860.
138. Ng, S.B., et al. (2011). Dysregulated microRNAs affect pathways and targets of biologic relevance in nasal-type natural killer/T-cell lymphoma. *Blood*. **118**, 4919-29.

139. Schneider, C., et al. (2014). MicroRNA 28 controls cell proliferation and is down-regulated in B-cell lymphomas. *Proc Natl Acad Sci U S A*. **111**, 8185-90.
140. Hell, M.P., et al. (2014). miR-28-5p promotes chromosomal instability in VHL-associated cancers by inhibiting Mad2 translation. *Cancer Res*. **74**, 2432-43.
141. Almanza, G., et al. (2013). Synthesis and delivery of short, noncoding RNA by B lymphocytes. *Proc Natl Acad Sci U S A*. **110**, 20182-7.
142. Kumar, P., et al. (2008). T cell-specific siRNA delivery suppresses HIV-1 infection in humanized mice. *Cell*. **134**, 577-86.
143. Lee, J., et al. (2012). T cell-specific siRNA delivery using antibody-conjugated chitosan nanoparticles. *Bioconjug Chem*. **23**, 1174-80.



## Curriculum Vitae

# Nathan Johnston

---

## **Education**

2012 – Present	Western University Master of Science in Pathology
2008 – 2012	Western University Bachelor of Medical Sciences Honours Specialization in Biochemistry of Infection and Immunity

## **Awards**

2013	2013-2014 CIHR Strategic Training Program in Cancer Research and Technology Transfer, London, ON
2012	2012-2013 Graduate Thesis Research Award Fund, Western University
2008-2012	Dean's Honours List, Western University
2008-2012	Western Continuing Admission Scholarship, Western University
2008-2012	Queen Elizabeth II Aiming for the Top Scholarship, Western University
2008	Governor General's Bronze Academic Medal, St. James Catholic High School

## **Work Experience**

2012 – 2014	Teaching Assistant, Biology 1002A/1002B Tom Haffie Western University – Department of Biology
2010 – 2011	Laboratory Research Assistant Dr. Kathleen Hill Western University – Department of Biology
2010, 2012	Sheep Flock Improvement Program Assistant/Genetics Assistant Delma Kennedy Ontario Ministry of Agriculture, Food and Rural Affairs

## **Publications**

- 2015      **Johnston, N.**, Zheng, X. and Min, W.P. An update on T cell targeted immunotherapies for metastatic melanoma. *Nat Rev Clin Oncol.* (2015). Submitted.
- Johnston, N.**, Zheng, X., Koropatnick, J., Zhang, X., Wang, H., Siu, K.S., Chen, R., Liu, Y. and Min, W.P. miR-28 and miR-107 silence programmed cell death-1 and reduce activation-induced apoptosis in CD4<sup>+</sup> T cells. *J Immunol.* (2015). Submitted.
- 2014      Zheng, X., Zhang, X., Ling, H., **Johnston, N.**, Chen, D., Siu, L., Luke, P., Jevnikar, A.M. and Min, W.P. Protection of renal function by perfusing donor organs with siRNA in kidney transplantation. *PLoS One.* (2014). Under revision.
- Wang, W., Chen, K., Liu, Q., **Johnston, N.**, Ma, Z., Zhang, F. and Zheng, X. Suppression of tumor growth by pleurotus ferulae ethanol extract through induction of cell apoptosis, and inhibition of cell proliferation and migration. *PLoS One.* eCollection (2014). Published.
- Zhang, X., Liu, Y., Zhang, G., Shi, J., Zhang, X., Zheng, X., Jiang, A.T., Zhang, Z.X., **Johnston, N.**, Siu, K.S., Chen, R., Lian, D., Koos, D., Quan, D. and Min, W.P. Synergic silencing of costimulatory molecules prevents cardiac allograft rejection. *J Transl Med.* **12**, 142 (2014). Published.
- Siu, K.S., Chen, D., Zheng, X., Zhang, X., **Johnston, N.**, Liu, Y., Yuan, K., Koropatnick, J., Gillies, E.R. and Min, W.P. Non-covalently functionalized single-walled carbon nanotube for topical siRNA delivery into melanoma. *Biomaterials.* **35**, 3435-42 (2014). Published.
- 2013      Zhou, L., Zang, G., Zhang, G., Wang, H., Zhang, X., **Johnston, N.**, Min, W., Luke, P., Jevnikar, A., Haig, A. and Zheng, X. MicroRNA and mRNA signatures in ischemia reperfusion injury in heart transplantation. *PLoS One.* eCollection (2013). Published.

## **Presentations**

- 2014      **Johnston, N.** MicroRNA regulation of PD1, TIM3 and BTLA: reverting T cell exhaustion to reduce melanoma development. 2014 Cancer Research and Technology Transfer Research & Education Day, Western University, London, ON. Poster Presentation.

**Johnston, N.** MicroRNA regulation of PD1, TIM3 and BTLA: reverting T cell exhaustion to reduce melanoma development. 2014 London Health Research Day, London Convention Centre, London, ON. Poster Presentation.

**Johnston, N.** MicroRNA regulation of PD1, TIM3 and BTLA: reverting T cell exhaustion to reduce melanoma development. 2014 Annual Pathology Research Day, Western University, London, ON. Poster Presentation.

2013 **Johnston, N.** miRNA regulation of PD1, TIM3 and BTLA: reverting T cell exhaustion to reduce melanoma. 2013 London Health Research Day, London Convention Centre, London, ON. Poster Presentation.

**Johnston, N.** miRNA regulation of PD1, TIM3 and BTLA: reverting T cell exhaustion to reduce melanoma. 2013 Annual Pathology Research Day, Western University, London, ON. Poster Presentation.

2012 **Johnston, N.** Assessment of Neurodegeneration in an Aged Rat Model of Alzheimer`s Disease. 2012 Anatomy and Cell Biology Research Day, Western University, London, ON. Poster Presentation.

### **Abstracts**

2013 Zhou, L., **Johnston, N.**, Zhang, X., Cheng, D., Sui, L., Luke, P., Jevnikar, A., Min, W. and Zheng, X. Regulation of microRNA in ischemia reperfusion injury in heart transplantation, The 2013 American Transplant Congress. Abstract number: B881.

### **Reports**

2012 Kennedy, D. and **Johnston, N.** Ontario GenOvis program annual report 2011. Ontario Ministry of Agriculture, Food and Rural Affairs (2012).